



CIVIL ENGINEERING STUDIES
Illinois Center for Transportation Series No. 14-014
UILU-ENG-2014-2014
ISSN: 0197-9191

IMPLEMENTATION OF AIMS IN MEASURING AGGREGATE RESISTANCE TO POLISHING, ABRASION, AND BREAKAGE

Prepared By
Enad Mahmoud
The University of Texas-Pan American

Eduardo Ortiz
Bradley University

Research Report No. FHWA-ICT-14-014

A report of the findings of
ICT-R27-129
**Implementation of AIMS in Measuring Aggregate Resistance to Polishing,
Abrasion, and Breakage**

Illinois Center for Transportation

May 2014

Technical Report Documentation Page

1. Report No. FHWA-ICT-14-014		2. Government Accession No.		3. Recipient's Catalog No.	
4. Title and Subtitle Implementation of AIMS in Measuring Aggregate Resistance to Polishing, Abrasion, and Breakage				5. Report Date May 2014	
				6. Performing Organization Code	
7. Author(s) Enad Mahmoud and Eduardo Ortiz				8. Performing Organization Report No. ICT-14-014 UILU-ENG-2014-2014	
9. Performing Organization Name and Address Illinois Center for Transportation Department of Civil and Environmental Engineering University of Illinois at Urbana-Champaign 205 N. Mathews Ave., MC-250 Urbana, IL 61801				10. Work Unit No. (TRAIS)	
				11. Contract or Grant No. R27-129	
12. Sponsoring Agency Name and Address Illinois Department of Transportation Bureau of Materials and Physical Research 126 E. Ash St. Springfield, IL 62704				13. Type of Report and Period Covered	
				14. Sponsoring Agency Code	
15. Supplementary Notes					
16. Abstract The feasibility of using the Micro-Deval apparatus along with the second-generation Aggregate Imaging System (AIMS) to develop a procedure for measuring aggregate polishing resistance, and to measure aggregate shape properties was investigated. Eleven aggregate sources from the state of Illinois and neighboring states were selected to develop an aggregate polishing experimental procedure using AIMS and Micro-Deval. AIMS was used to measure aggregate shape properties with a special focus on aggregate angularity and surface texture, while Micro-Deval provided the needed polishing/degradation. Mathematical, statistical, and rate of texture loss analysis indicated that all aggregate sources reached terminal texture at 210 minutes or less. Aggregate angularity followed the same trend, and terminal angularity was achieved at 210 minutes or less. As the polishing procedure was finalized, aggregate shape properties were tested for 77 aggregate sources. Shape properties were measured before polishing and after polishing in Micro-Deval at 105 and 210 minutes, and a database was developed using Microsoft Excel. The research team also studied the number of aggregate particles that must be scanned in AIMS. Random sub-sampling and asymptotic analyses were conducted and it was concluded that 120 particles were required. This finding was further evaluated by manual sampling of 120 aggregate particles. The manual sampling proved that 120 particles were enough for AIMS angularity and texture measurements.					
17. Key Words Aggregate, Polishing, Friction, AIMS, Imaging, Angularity, Texture			18. Distribution Statement No restrictions. This document is available to the public through the National Technical Information Service, Springfield, Virginia 22161		
19. Security Classif. (of this report) Unclassified		20. Security Classif. (of this page) Unclassified		21. No. of Pages 52	22. Price

ACKNOWLEDGMENTS

This publication is based on the results of ICTR27-129, **Implementation of AIMS in Measuring Aggregate Resistance to Polishing, Abrasion, and Breakage**. ICTR27-129 was conducted in cooperation with the Illinois Center for Transportation; the Illinois Department of Transportation, Division of Highways; and the U.S. Department of Transportation, Federal Highway Administration.

The research team appreciates the contribution of the members of the Technical Review Panel (TRP):

- Sheila Beshears (TRP Chair, IDOT)
- Scott Hughes (IDOT)
- Daniel McGee (IDOT)
- Garry Millhoff (IDOT)
- Matthew Mueller (IDOT)
- LaDonna Rowden (IDOT)
- Brian Pfeifer (FHWA)

The research team also extends special appreciation to Dr. Erol Tutumluer and Mr. Maziar Moaveni from the University of Illinois at Urbana-Champaign, for their input and assistance during the data collection phase.

DISCLAIMER

The contents of this report reflect the view of the authors, who are responsible for the facts and the accuracy of the data presented herein. The contents do not necessarily reflect the official views or policies of the Illinois Center for Transportation, the Illinois Department of Transportation, or the Federal Highway Administration. This report does not constitute a standard, specification, or regulation.

MANUFACTURERS' NAMES

Trademark or manufacturers' names appear in this report only because they are considered essential to the object of this document and do not constitute an endorsement of product by the Federal Highway Administration, the Illinois Department of Transportation, or the Illinois Center for Transportation.

EXECUTIVE SUMMARY

The main objectives of this research were to study the feasibility of using the Micro-Deval apparatus along with the second-generation Aggregate Imaging System (AIMS) to develop a procedure for measuring aggregate polishing resistance, and to measure aggregate shape properties using AIMS. Additionally, the new Enhanced University of Illinois Aggregate Image Analyzer (E-UIAIA) was also used as a second imaging system to capture the rate and magnitude of angularity as well as texture loss under the effect of Micro-Deval.

The research team, in coordination with IDOT's Bureau of Materials and Physical Research (BMPR), selected 11 aggregate sources from the state of Illinois and neighboring states to develop an aggregate polishing experimental procedure using AIMS and Micro-Deval. AIMS was used to measure aggregate shape properties with a special focus on aggregate angularity and surface texture, while Micro-Deval provided the needed polishing/degradation. The Micro-Deval polishing time required for the aggregate to reach terminal polishing was determined. Therefore, eight samples of each source were polished at: 15, 30, 45, 60, 75, 90, 105, and 180 minutes. A modified one-aggregate size Micro-Deval procedure was implemented. Mathematical and statistical analyses showed that not all 11 aggregates reached terminal polishing and that 210 minutes of polishing were sufficient. An extra sample was then polished from each source at 210 minutes in the Micro-Deval for verification purposes. Mathematical, statistical, and rate of texture loss analyses indicated that all aggregate sources reached terminal texture at 210 minutes or less. Aggregate angularity followed the same trend, and terminal angularity was achieved at 210 minutes or less in the modified Micro-Deval procedure.

As the polishing procedure was finalized, aggregate shape properties were tested for 77 aggregate sources. Shape properties were measured before and after polishing in Micro-Deval at 105 and 210 minutes, and a database was developed using Microsoft Excel. The aggregate polishing characteristics can be described using the following mathematical expression:

$$Texture(t) = a + b * e^{-c*t}$$

The research team also studied the number of aggregate particles that must be scanned in AIMS. Random sub-sampling and asymptotic analyses were conducted and it was concluded that 120 particles were required. This finding was further evaluated by manual sampling of 120 aggregate particles. The manual sampling proved that 120 particles were enough for AIMS angularity and texture measurements.

Finally, the research team recommended the collection of additional aggregate polishing characteristics of more aggregate sources with the current VST procedure to allow for future comparisons and prospective policy changes.

CONTENTS

- CHAPTER 1 INTRODUCTION 1**
 - 1.1 Background and Relevant Literature..... 1**
 - 1.2 Objectives of the Study 3**
 - 1.3 Research Approach 3**
 - 1.3.1 Task 1—Identification of Aggregate Sources..... 3
 - 1.3.2 Task 2—Measurement of the Shape Properties of Aggregate Samples 3
 - 1.3.3 Task 3—Database Compilation 3
 - 1.3.4 Task 4—Development of Experimental Methods to Measure Aggregate Resistance to Polishing, Abrasion, and Breakage 3
 - 1.3.5 Task 5—Measurement of Aggregate Shape Properties after Micro-Deval (Terminal Texture)..... 4
 - 1.3.6 Task 6—Recommendations and Testing Procedure..... 4
 - 1.3.7 Task 7—Preparation and Revision of Final Report..... 4
- CHAPTER 2 EXPERIMENTAL PROGRAM 5**
 - 2.1 Materials 5**
 - 2.2. Equipment 5**
 - 2.2.1 Second-Generation Aggregate Imaging System (AIMS)..... 5
 - 2.2.2 Enhanced University of Illinois Aggregate Image Analyzer (E-UIAIA)..... 7
 - 2.2.3 Micro-Deval 10
 - 2.3 Testing Procedures..... 11**
 - 2.3.1 Task 2 11
 - 2.3.2 Task 4 11
- CHAPTER 3 RESULTS AND ANALYSES..... 12**
 - 3.1 Minimum Number of Aggregate Particles 12**
 - 3.1.1 Selection of Samples..... 12
 - 3.1.2 Random Sub-Samples Method..... 13
 - 3.1.3 Asymptotic Analysis 17
 - 3.1.4 Manual Random Sampling 19
 - 3.2 Terminal Polishing..... 22**
 - 3.2.1 Stage 1: Preliminary Evaluation..... 22
 - 3.2.2 Stage 2: Extended Polishing Time..... 28
 - 3.2.3 Stage 3: Terminal Polishing..... 34
 - 3.2.4 Stage 4: Procedure Simplification..... 40
 - 3.2.5 Stage 5: Procedure Extension 42
 - 3.3 AIMS Database 45**

CHAPTER 4 SUMMARY AND IMPLEMENTATION RECOMMENDATIONS	47
4.1 Summary	47
4.2 Implementation Recommendations	47
4.2.1 Polishing Procedure	47
4.2.2 Database.....	48
4.2.3 Procedure Validation	48
REFERENCES	49

CHAPTER 1 INTRODUCTION

1.1 BACKGROUND AND RELEVANT LITERATURE

Aggregate properties impact several aspects of asphalt pavement performance. The performance parameters affected by aggregate properties are permanent deformation, fatigue cracking, frictional resistance, thermal cracking, and raveling (Kandhal and Parker 1998). The main aggregate properties that are linked to asphalt pavement performance are gradation and size, particle shape and surface texture, porosity, cleanliness, toughness and abrasion resistance, durability and soundness, expansive characteristics, polish and frictional characteristics, and mineralogy and petrography (Kandhal and Parker 1998). Additionally, the shape properties of aggregate particles significantly affect the performance of the unbound/bound layers of highway/airfield pavements as well as railroad ballast under dynamic traffic loading in terms of shear strength, modulus and permanent deformation characteristics (Kandhal and Parker 1998; Masad et al. 2007; Tutumluer and Pan 2008; Indraratna and Salim 2005). The influence of aggregate shape characteristics on asphalt pavement performance was highlighted in a research study conducted under National Cooperative Highway Research Program NCHRP 4-30A (Masad et al. 2005). The study revealed that shape, angularity, and texture are all significant characteristics for predicting pavement performance. In another research study (McGahan 2005), comprehensive statistical analyses were conducted to investigate relationships between aggregate shape characteristics and asphalt mix mechanical properties. The study showed that aggregate shape characteristics impact the mechanical properties of asphalt mixes.

Frictional resistance, also known as skid resistance, is considered one of the most important performance parameters of asphalt pavement. The importance of pavement frictional resistance stems from its impact on travel safety, and thus a minimum acceptable safe limit must be maintained (Bloem 1971). Skid resistance of asphalt pavements depends primarily on the microtexture and macrotexture of the surface (Dahir 1979). Microtexture depends primarily on aggregate shape characteristics, while macrotexture is a function of the mix properties, compaction method, and aggregate gradation (Kandhal and Parker 1998; Crouch et al. 1995; Luce et al. 2007; Forster 1989). Skid resistance of asphalt pavement surfaces is presumably adequate right after pavement construction and after the pavement is opened to traffic; aggregates that resist polishing and wear are therefore desired (Bloem 1971). Aggregate polishing resistance is often tested to evaluate aggregate materials before they are used in hot mix asphalt (HMA) surface courses.

Aggregate resistance to abrasion and breakage, also known as degradation, is another important aggregate property that influences several HMA performance parameters. Abrasion is defined as the loss of aggregate angularity, while breakage refers to particles fracturing. Aggregates are exposed to degradation during production, transportation, and construction (mixing and compaction), before the pavement is put into service. Several types of forces such as attrition, impact, and grinding are imposed on the aggregate particles at different stages, including production at the quarry/plant (Page et al. 1997), transportation to job site, and compaction during construction. These factors, along with in-service dynamic traffic loading and environmental effects, cause "aggregate degradation." Aggregate degradation affects gradation; thus, the mix produced in the field differs from the mix designed in the laboratory (Wu et al. 1998). Initially, contact forces provide the energy required for the relocation/rearrangement of particles and therefore aggregate particles are subjected to contact forces when adjusting to their new locations, which may eventually cause breakage and wear at the points of contact (Moavenzadeh and Goetz 1963). Mineralogical and petrographic properties as well as initial gradations are crucial factors that control the magnitude and trend of aggregate degradation. Several studies investigated the characterization of aggregate degradation and its effect on the bearing capacity

of unbound/bound layers in terms of the change in size distribution or decrease in coarse to fine fraction ratio (Pintner et al. 1987; Gatchalian et al. 2006; Lynn et al. 2007). However, only a few research studies examine the effect of aggregate degradation on altering shape characteristics of the aggregates. Aggregate degradation can cause particles to lose their angularity and surface texture or become more rounded and spherical, which results in changing the void ratio or packing properties and, ultimately, influencing the performance. The lack of research in this area may be possibly attributed to the absence of a unified standard procedure for rapid and quantitative measurement of the shape properties of aggregate particles. New generations of asphalt mixes, such as Stone Matrix Asphalt (SMA), transfer stresses within the aggregate structure, thus producing high stresses at the stone-to-stone contact points which might cause aggregate fracture and, consequently, affect the performance of the mix (Gatchalian 2005).

The methods used for measuring aggregate shape characteristics are classified into two categories: direct and indirect (Kandhal et al. 1991; Janoo 1998; Chowdhury et al. 2001). In a direct method, particle shape characteristics are measured, described, or quantified through direct measurement of individual aggregate particles, whereas the indirect methods measure particle shape characteristics as a bulk property of aggregate particles. Direct methods range from simple, visual methods to mechanical devices and sophisticated advanced imaging systems. Several imaging systems are currently available for measuring aggregate shape characteristics (Barksdale et al. 1991; Kuo et al. 1996; Masad et al. 1999a, 1999b; Brzezicki and Kasperkiewicz 1999; Weingart and Prowell 1999; Maertz and Zhou 2001; Tutumluer et al. 2000, Li et al. 1993; Wilson and Klotz 1996; Yeggoni et al. 1994; Masad et al. 2000, 2001; Kuo and Freeman 2000; Rao et al. 2002; Hryciw and Raschke 1996; Wang and Lai 1998; Masad and Button 2000; Masad et al. 2001). With the introduction of the software and hardware components of advanced machine vision technology, it has become possible to measure the shape properties of aggregates in a quantitative and objective manner. A variety of imaging-based aggregate morphological indices have been developed and linked to material strength and deformation properties (Al-Rousan et al. 2007; Wang et al. 2012). Although none of these methods has yet been recommended as a standard testing procedure, extensive research has been performed to evaluate the performance and reliability of these techniques for characterizing the shape properties of aggregate productions (Mahmoud et al. 2010; Pan and Tutumluer 2010). According to NCHRP 4-30 study (Masad et al. 2007), flat and elongated ratio (FER), angularity index (AI), and surface texture index (STI) measured with the Aggregate Imaging System (AIMS) and the University of Illinois Aggregate Image Analyzer (UIAIA) are recognized as the most validated indices to represent the aggregate shape properties and their linkage to field performance.

During the last decade, researchers have started using imaging-based measurement of aggregate shape properties along with laboratory degradation resistance testing methods to quantify the magnitude and trend of aggregate degradation. UIAIA has been combined with Los Angeles abrasion and impact test (ASTM C535) to measure the effect of abrasion and impact forces on shape properties during the degradation process (Boler et al. 2012). Recently, several studies evaluated the use of the Micro-Deval test along with imaging systems to measure the effect of the test on aggregate shape characteristics (Mahmoud 2005; Luce 2006; Lane et al. 2011). Mahmoud and Masad (2007) used AIMS along with the Micro-Deval test to measure aggregate polishing, abrasion, and breakage. Aggregate polishing was characterized at several Micro-Deval polishing times by measuring the texture index, while abrasion and breakage were characterized by angularity and weight loss measurements. The study illustrated the capability of Micro-Deval along with AIMS texture measurements to polish aggregates, and measure aggregate polishing characteristics: initial texture, rate of polishing, and terminal texture were successfully estimated. More recent studies have shown the ability of imaging techniques to evaluate the level of degradation on site by measuring the shape properties of the aggregate samples collected from asphalt plants or in-service, unbound aggregate layers (Singh et al. 2013; Moaveni et al. 2013).

Two imaging systems will be evaluated in this study: Aggregate Imaging Measurement System (AIMS) and the recently Enhanced University of Illinois Aggregate Image Analyzer (E-UIAIA); both systems are currently used to quantify aggregate shape properties for several pavement and railroad track applications. Furthermore, both systems have undergone vast improvements during the past five years and a second generation of both systems is currently available.

1.2 OBJECTIVES OF THE STUDY

This study has two main objectives:

- Measure aggregate shape characteristics of aggregate sources from the state of Illinois and neighboring states using AIMS and E-UIAIA systems
- Study the feasibility of implementing AIMS, along with the Micro-Deval equipment, to measure aggregate resistance to polishing, abrasion, and breakage

1.3 RESEARCH APPROACH

The objectives of this research study were accomplished by performing the following tasks:

1.3.1 Task 1—Identification of Aggregate Sources

The research team worked with IDOT personnel to identify aggregate sources of different mineralogy throughout the state of Illinois and neighboring states. A total of 77 aggregate sources were identified. Two samples from each source were collected for testing. Each sample consisted of 750 g passing the 12.5 mm sieve and retained on the 9.5 mm sieve. Eleven sources were selected for the terminal polishing study, and nine samples were used from each source to establish the aggregate polishing curves.

1.3.2 Task 2—Measurement of the Shape Properties of Aggregate Samples

The research team purchased the Aggregate Imaging Measurement System (AIMS) and borrowed the Micro-Deval equipment from IDOT. The equipment is currently located in the aggregate laboratory at IDOT. Each sample was washed, dried, and scanned with AIMS and E-UIAIA to measure its shape properties. The scanned samples were then polished in Micro-Deval, and the aggregate particles were then washed, sieved, and dried before scanning with AIMS and E-UIAIA. The weight loss caused by Micro-Deval polishing was also recorded.

1.3.3 Task 3—Database Compilation

A database of aggregate properties was compiled and delivered to IDOT in Microsoft Excel format. The database included the aggregate shape properties measured before and after the Micro-Deval test and the weight loss caused by Micro-Deval polishing.

1.3.4 Task 4—Development of Experimental Methods to Measure Aggregate Resistance to Polishing, Abrasion, and Breakage

Eleven sources were selected by the Technical Review Panel (TRP) to be used for developing an experimental procedure for measuring aggregate resistance to polishing, abrasion, and breakage. AIMS and E-UIAIA were used to measure aggregate texture while the Micro-Deval test was used as the polishing mechanism. The effect of polishing time in the Micro-Deval was examined to determine the time required to achieve terminal texture value. The selected sources were subjected to Micro-Deval polishing for 15, 30, 45, 60, 75, 90, 105, 180, and 210 minutes; a different sample was used for each time interval. Statistical analysis was conducted to select the minimum number of time intervals required to capture the change in texture behavior.

1.3.5 Task 5—Measurement of Aggregate Shape Properties After Micro-Deval (Terminal Texture)

Based on the results of the analysis conducted in Task 4, samples of the sources selected in Task 1 were polished in Micro-Deval for a period of time (number of revolutions) sufficient to achieve terminal texture. The resulting data was added to the database developed in Task 4. With the conclusion of this Task, aggregate shape properties before Micro-Deval (BMD), after Micro-Deval (AMD), and AMD-terminal were documented for all aggregate sources.

1.3.6 Task 6—Recommendations and Test Procedures

Recommendations and test procedures are outlined in this report.

1.3.7 Task 7—Preparation and Revision of Final Report

The final report explains the methodology, findings, and conclusions of this study.

CHAPTER 2 EXPERIMENTAL PROGRAM

2.1 MATERIALS

The aggregate materials used in this study were selected from a wide range of mineralogical properties and various quarries in different geographical regions in the state of Illinois and neighboring states. All aggregate materials were washed, oven dried, and sieved to obtain particle sizes passing the ½ in. (12.5 mm) sieve and retained on the 3/8 in. (9.5 mm) sieve. 77 sources were tested for Task 2, while eleven sources were tested for Task 4. Table 3.1 lists the types and designations of all aggregate materials tested in Task 4. Previous research has shown the effect of using single versus multiple aggregate samples (Mahmoud and Masad 2007) and proved that the two procedures would yield similar results. However, multiple aggregate samples were used from each source at different degradation times to ensure consistency of initial gradation and aggregate weight for each set of Micro-Deval tests.

Table 2.1 Aggregate Material Types, Designations, and Geology

Aggregate ID	Aggregate Description	Geology
FP1	Limestone	Pennsylvanian/Bond/Millersville
FP2	Limestone	Mississippian/Salem
FP3	Limestone	Ordovician/Galena
FP4	Silurian Dolomite (Reef Formation)	Silurian/Racine
FP5	Silurian Dolomite	Silurian/Racine/Joliet
FP6	Crushed Gravel	Henry Formation, Wisconsinin Glacial Till
FP7	Chert Gravel	Maramec River Gravel, 99% Chert
FP8	Steel Slag	Steel Slag
FP9	ACBF Slag	Air-Cooled Blast Furnace Slag
FP10	Quartzite	Lower Proterozoic Quartzite (Baraboo Formation)
FP11	Sandstone	Mississippian/Rosiclare Sandstone

2.2. EQUIPMENT

2.2.1 Second-Generation Aggregate Imaging System (AIMS)

AIMS determines the shape characteristics of aggregate through image processing and analysis techniques. It consists of a computer-automated unit that includes a circular measurement tray. The system is also equipped with top lighting, back lighting, and a camera unit (Figure 2.1). Coarse aggregates are placed in the trough of the circular tray; the tray is rotated to move the aggregates under the camera unit, which is fixed in the x and y directions. As the backlit tray moves, the aggregates move under the camera and several images are captured for measuring angularity. The positions of aggregates are recorded so the camera can return to the centroid of the particles for texture image acquisition. AIMS configuration uses a removable tray for each aggregate size to position the particles properly for imaging and to facilitate materials loading. Trays of different colors highlight

the contrast between the material particles and the background. The shape characteristics of aggregate: shape, angularity, and surface texture are produced by AIMS software, which analyzes the aggregate images. The shape is described by a 2-D form and 3-D form (Sphericity). Aggregate angularity is represented by measuring the irregularity of a particle surface from a black and white image using the gradient method (angularity index). The texture index is obtained by analyzing grayscale images captured on the aggregate surface using a wavelet analysis method. The dimensions of the aggregates are obtained during angularity and texture scans. The black and white angularity images are used to measure the x and y dimensions, while the depth is obtained as the camera unit focuses on the particle surface while scanning for surface texture grayscale images (Masad et al. 2007). AIMS software results for each individual particle are listed along with essential statistical values for the scanned sample, such as the mean, standard deviation, and cumulative distribution of measurements for each aggregate shape property (Al-Rousan 2004; Gates 2010; Gates et al. 2011).



Figure 2.1 Second-generation Aggregate Imaging Measurement System (AIMS).

This section provides a short summary about the calculation of individual shape indices using AIMS.

2.2.1.1 Flat and Elongated Ratio (FER)—Sphericity

According to ASTM D4791, the FER of an aggregate particle is defined as the ratio of the maximum dimension to minimum dimension of the particle. Projections of a particle placed on the lighting table are captured by the camera in AIMS and used to generate the binary image. Eigenvector analysis (Fletcher et al. 2003) on binary images identifies the major and minor axes of the particle. The third dimension or depth of particle is measured by determining the distance between the camera's lens and surface of particle relative to the original location of the camera. The image processing algorithm sorts the three dimensions and identifies the maximum, minimum, and intermediate particles sizes. Sphericity can be computed using Equation 1 (Al-Rousan et al. 2005).

$$Sphericity = \sqrt[3]{\frac{d_s \times d_l}{d_l^2}} \quad (1)$$

where

d_L = Longest dimension
 d_I = Intermediate dimension
 d_S = Shortest dimension

2.2.1.2 Angularity Index (AI)

The gradient method is used as the image processing technique for AI measurements. The gradient method calculates the inclination of gradient vectors on particle boundary points from the x-axis (horizontal axis in an image). The average change in the inclination of the gradient vectors is considered an indicator of angularity and can be calculated using Equation 2 (Al-Rousan et al. 2005).

$$\text{Angularity Index} = \frac{1}{\frac{N-3}{3}-1} \sum_{i=1}^{N-3} |\theta_i - \theta_{i+3}| \quad (2)$$

where

θ_i = inclination of gradient vectors on particle boundary point i
 i = denotes the i^{th} point on the boundary of a particle
 N = total number of points on the boundary

The average, rather than the summation, is considered in Equation 2 so that angularity calculation is not affected by particle size. The step size used for calculating gradients is three because it minimizes the effect of noise created during image acquisition on the results (Masad 2003).

2.2.1.3 Surface Texture Index (STI)

STI is measured using the wavelet technique. Texture details are identified in the horizontal, vertical, and diagonal directions in three separate images. The texture index at the desired decomposition level is considered the arithmetic mean of the squared values of the wavelet coefficients for all three directions as illustrated in Equation 3 below (Masad 2003; Al-Rousan et al. 2005).

$$\text{Texture Index} = \frac{1}{3N} \sum_{i=1}^3 \sum_{j=1}^N [D_{ij}(x, y)]^2 \quad (3)$$

where

N = Number of coefficients
 $i = 1, 2, 3$ for the three directions of texture
 j = Wavelet coefficient index
 D = Wavelet coefficient

2.2.2 Enhanced University of Illinois Aggregate Image Analyzer (E-UIAIA)

The UIAIA (Figure 2.2) system was developed by Dr. Erol Tutumluer, Professor of Civil and Environmental Engineering at the University of Illinois at Urbana-Champaign. The system is based on capturing three projections of aggregate particles while moving on a conveyer belt; the projections are then used to reconstruct a three-dimensional representation of aggregate particles. The system provides information on gradation, form, angularity, texture as well as surface area and volume using the measured dimensions directly without any assumptions or idealization of the particle shape (Rao et

al. 2002). Recently, an enhanced second-generation UIAIA has been designed and manufactured at the University of Illinois with many improvements over the original system. Figure 2.2 features an aggregate particle with three orthogonal views captured using high resolution progressive scan digital color cameras. These views are used to quantify imaging-based morphological indices. Unlike the old version of UIAIA, which only was capable of capturing black and white images, the new system is equipped with three high resolution (1,292 x 964 pixels) Charge Coupled Device (CCD) progressive scan cameras to capture digital color images of aggregate particles. Because black and white images are generally used for texture analysis, the majority of texture details are lost when gray scale images are converted into black and white. Therefore, the influence of natural color variation of the aggregate on grayscale intensities, which directly affects the texture, needs to be addressed by using colored rather than black and white images (Al-Rousan et al. 2007). An advanced color thresholding scheme is used in the processing software of E-UIAIA. Different types of mineral aggregates with vast 16 colors can be scanned with this system. Four LED illumination lights with dimmer controls assist the operator to achieve the best contrast and capture the sharpest aggregate images possible by optimizing light intensity and minimizing shadows. An enhanced calibration adjustment interface also changes the spatial resolution corresponding to the size of aggregate particles scanned by using the zooming capability of the camera lenses. E-UIAIA software exports the computed shape indices to a MS Excel file for further post-processing and statistical analysis. The system can be calibrated using spherical balls to adjust the spatial resolution of aggregate sizes ranging between 3 in. (76.2 mm) to 0.187 in. (4.75 mm). A user-friendly shape property analysis software has been developed to measure AI, STI, FER as well as the surface area (SA) and volume (V) of individual particles (Moaveni et al. 2013).

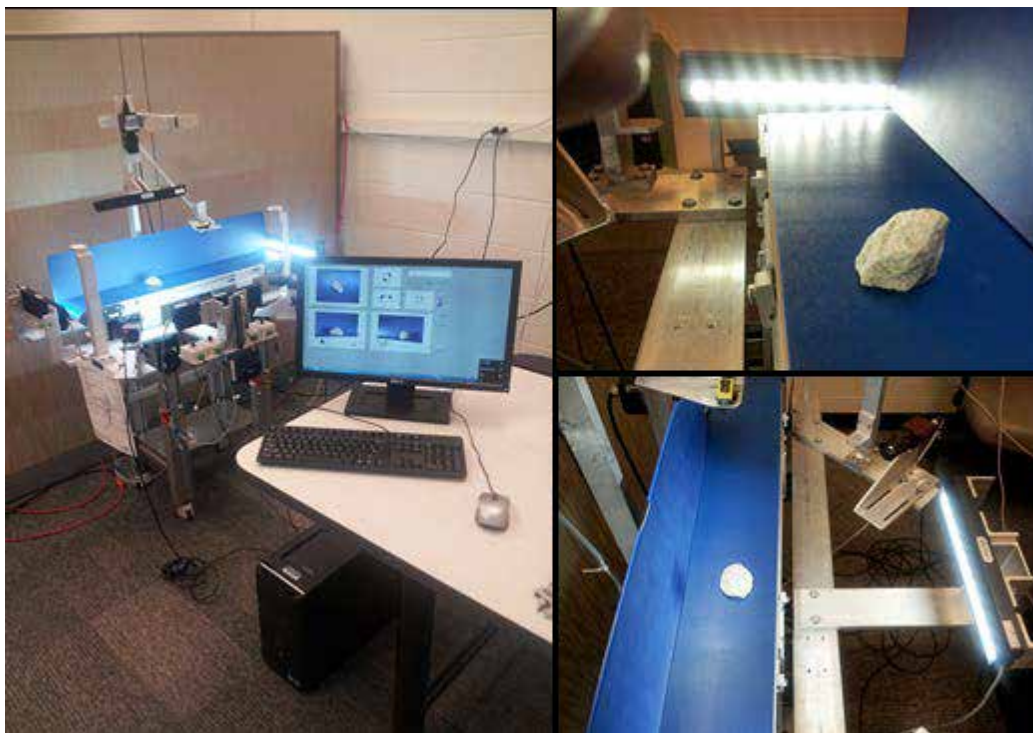


Figure 2.2 Enhanced University of Illinois Aggregate Image Analyzer (E-UIAIA).

This section presents a brief background of the methodology used in E-UIAIA for particle morphology analysis.

2.2.2.1 Flat and Elongated Ratio (FER)

The longest and shortest dimensions are determined using the three views of an aggregate particle. After a number of particles are tested, the FER values (ratio of longest to shortest dimension) are averaged for a certain aggregate sample (Tutumluer et al. 2000).

2.2.2.2 Angularity Index (AI)

First, the coordinates of the profile are extracted to estimate the profile of each 2-D image of a particle. Second, the particle outline is estimated by an n-sided polygon as shown in Figure 2.3. Previous research showed that choosing an optimum value of $n = 24$ points around the perimeter of particle would yield the best performance of the algorithm in terms of detecting the largest AI differences between crushed and uncrushed aggregate (Tutumluer et al. 2000; Rao et al. 2002). The angle subtended at each vertex of the polygon is then computed. A relative change in slope of the n sides of the polygon is subsequently approximated by calculating the change in angle a at each vertex relative to the angle in the preceding vertex. The frequency distribution of the changes in the vertex angles is established in 10-degree class intervals. Finally, the number of occurrences in a certain interval and the magnitude are related to the angularity of the particle profile.

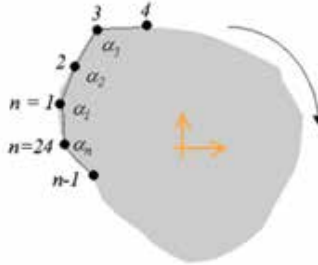


Figure 2.3 Estimating an aggregate particle with an n-sided polygon.

Equation 4 represents the formula used for computing the *angularity index* of each projected image.

$$\text{Angularity Index} = \sum_{e=0}^{170} e \times P(e) \quad (4)$$

where

e = the starting angle value for each 10-degree class interval

$P(e)$ = the probability that change in angle a has a value ranging between e and $(e+10)$

The *angularity index* has the degree unit. The final AI value is the area-weighted average value of the individual *angularity index* values determined from three views (front, top, and side images).

2.2.2.3 Surface Texture Index (STI)

Image filtering with “dilation and erosion” operations is a fundamental concept in morphological image processing and has been implemented in E-UIAIA to measure the STI of aggregate particles. Dilation is an operation that grows or thickens the object in an image while erosion shrinks or makes them thinner (Gonzalez et al. 2009). Erosion cycles followed by the same number of dilation cycles tend to smooth the surface of a particle by trimming the peaks and corners and patching the sharp dents on the boundary. The imaging pixel count-based area difference of the 2-D image before and after the erosion and dilation cycles of the same number of cycles is directly related to the surface micro-irregularities (Pan 2006). Equation 5 is used to compute the *surface texture index* of a 2-D aggregate particle image.

$$\text{Surface Texture Index} = \frac{A_1 - A_2}{A_1} \times 100 \quad (5)$$

where

A_1 = Initial area (in pixels) of the 2-D image of particle

A_2 = Area (in pixels) of the particle after performing a sequence of “ n ” cycles of erosion followed by “ n ” cycles of dilation

The optimal value of n , which is equal to 20, is considered the point where the *surface texture index* of a set of smooth surface coarse aggregates is recognized as significantly separated from the *surface texture index* of a set of rough surface coarse aggregates (Pan 2006). The final STI value is an area-weighted average value of its individual image *surface texture index* values determined from three views (front, top, side images).

2.2.3 Micro-Deval

Several test methods measure aggregate abrasion, polishing, and impact. The Los Angeles abrasion and impact test is the most widely used method for measuring aggregate resistance to abrasion and aggregate toughness (Kandhal and Parker 1998). Another test that has been used for measuring abrasion resistance is the Micro-Deval test. The Micro-Deval test measures aggregate resistance to abrasion and aggregate durability. Abrasion is simulated by the interaction of aggregate particles and steel balls in presence of water (Cooley and James 2003). Several research studies compared the Micro-Deval and L.A. abrasion and impact tests and concluded that the Micro-Deval gives a better simulation of field conditions (Rogers 1998) and induces more tumble than impact (Meininger 2004) compared with the L.A. test. The LA test is believed to be more of an impact test (Lane et al. 2000) and it has poor correlation with field performance (Senior and Rogers 1991). Therefore, several researchers and DOT's are considering the Micro-Deval test as part of aggregate testing and quality control/assurance procedures (QC/AC). In the Micro-Deval test, an oven-dried sample of 1500 ± 5 g with standard gradation is initially soaked in water for a minimum of 1 hour; the sample is then placed in Micro-Deval jar with 2000 ml of water and an abrasive charge consisting of 5000g stainless steel balls of 9.5 mm diameter. The jar, aggregate, water, and steel balls charge are then revolved at a specific speed for a specific time or to a specific number of revolutions based on the gradation used. The sample is then washed and oven dried at $110 \pm 5^\circ\text{C}$ to constant mass. The Micro-Deval weight loss, represented as the percentage by mass of the original sample, is the amount of material passing the 1.18-mm sieve.

$$\text{Weight loss} = \frac{A - B}{A} \times 100 \quad (6)$$

where

A = Mass recorded before test

B = Mass recorded after test

2.3 TESTING PROCEDURES

2.3.1 Task 2

Aggregate resistance to degradation was measured based on the following procedure:

- Two aggregate samples were obtained from the selected source: each sample was 750 g passing the 1/2 in. sieve and retained on the 3/8 in. sieve
- The aggregate particles were scanned with AIMS to obtain initial aggregate shape properties – Before Micro-Deval (BMD)
- The Micro-Deval drum was filled with 750 grams of aggregate materials
- The drum was charged with 5,000 grams of 9.5 mm diameter steel balls and 2 liters of water
- The aggregate sample was subjected to a target degradation time:
 - § Sample 1: 105 minutes
 - § Sample 2: 210 minutes
- The sample was washed on top of the No. 16 sieve size and the steel balls were removed
- The aggregate shape measurements associated with each degradation time for the portion retained on the 3/8 in. sieve – After Micro-Deval (AMD) were recorded

2.3.2 Task 4

Aggregate polishing curves were developed using the following procedure:

- Nine aggregate samples were obtained from the selected source: each sample was 750 g passing the 1/2 in. sieve and retained on the 3/8 in. sieve
- The aggregate particles were scanned with AIMS and E-UIAIA to obtain initial aggregate shape properties – Before Micro-Deval (BMD)
- The Micro-Deval drum was filled with 750 grams of aggregate materials
- The drum was charged with 5,000 grams of 9.5 mm diameter steel balls and 2 liters of water
- The aggregate sample was subjected to a target degradation time: 15, 30, 45, 60, 75, 90, 105, 180, and 210 minutes
- The sample was washed over a No. 16 sieve size and the steel balls were removed
- The aggregate shape measurements associated with each degradation time for the portion retained on the 3/8 in. sieve – After Micro-Deval (AMD) were recorded
- The aggregate texture was plotted with time in Micro-Deval to obtain the polishing curve

CHAPTER 3 RESULTS AND ANALYSES

3.1 MINIMUM NUMBER OF AGGREGATE PARTICLES

The aggregate samples tested with AIMS for obtaining their shape properties contained 300 to 400 particles. This section summarizes the approach used to determine the required number of particles for scanning with AIMS.

3.1.1 Selection of Samples

Six samples were selected from the results obtained from AIMS scanning in Tasks 2 and 4. The selected samples cover a wide range of angularity and texture. Figure 3.1 shows the angularity and texture range for the selected aggregates. The index values are listed in Table 3.1.

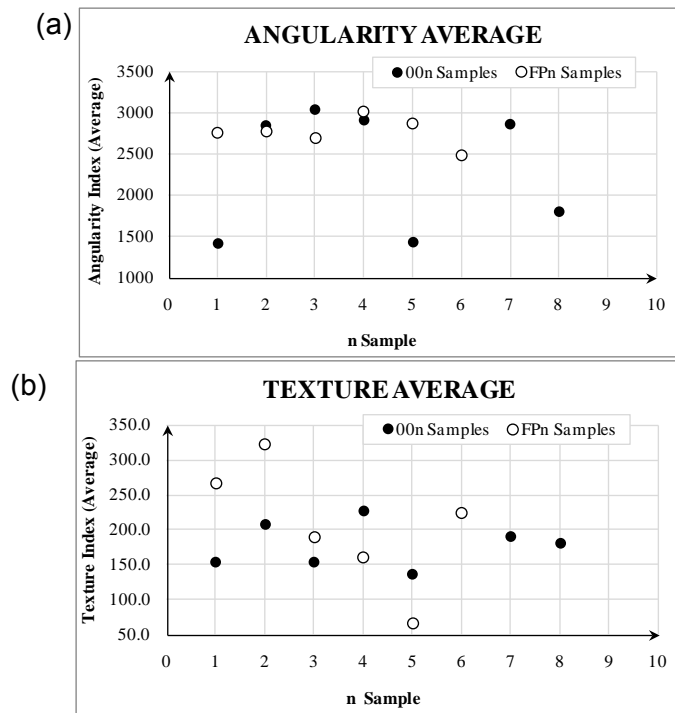


Figure 3.1. Variations of AIMS shape properties for different samples.

Table 3.1. AIMS Shape Properties for the Samples Selected

SELECTED SAMPLES	AVERAGES	
	ANGULARITY	TEXTURE
Sample 001	1409.9	154.4
Sample 002	2843.1	207.8
Sample 003	3028.8	153.2
Sample 005	1434.0	136.4
Sample FP2	2778.7	321.8
Sample FP5	2868.9	67.1

3.1.2 Random Sub-Samples Method

3.1.2.1 Random Sub-Samples Technique

The random selection was performed by using random numbers to select different values of texture and angularity. The random selections were obtained from the files generated by AIMS once a shape analysis was completed. Twenty groups of different sub-sample sizes were generated. Each group consisted of one thousand sub-samples with the sizes increasing by 10 particles in every consecutive group. The size of the starting sub-sample was 10 particles and therefore the maximum size of the sub-sample was 200 particles as shown in Table 3.2.

Table 3.2. Arrangement for the Statistical Analyses

GROUP	SUB-SAMPLES				
	Size	# Generated			
1	10	1	2	...	10
2	20	1	2	...	10
...
20	200	1	2	...	10

The arrangement described above allows for tracking the convergence of measured properties. The averages of the shape properties for the particles (50 - 500) in every sample were compared with the averages of the 20 groups of 10 randomly selected sub-samples. Standard errors were also compared in a similar fashion.

3.1.2.2 Random Sub-Sample Results

The average of every group (with different sub-sample size) was compared with the average of the entire sample. Whenever the average of a specific group was equal to the average of the entire sample, the group sub-sample size was recorded. This sub-sample size was the minimum required to represent the entire sample accurately. The confidence interval (CI) was represented by two standard

errors above and under the group average value. Figure 3.2 shows the results for the angularity data and Figure 3.3 represents the texture index results.

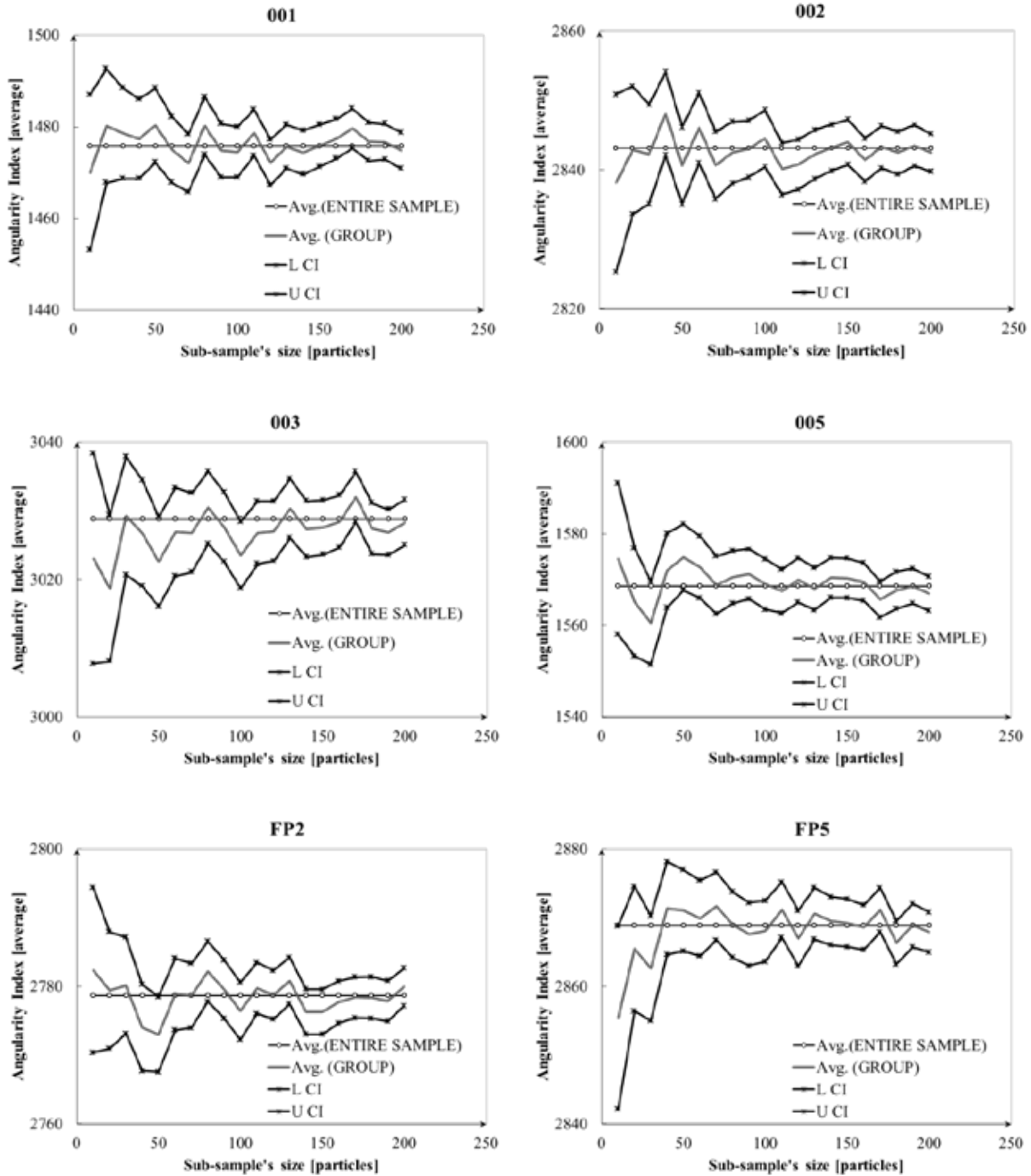


Figure 3.2. Average distributions of *angularity* index.

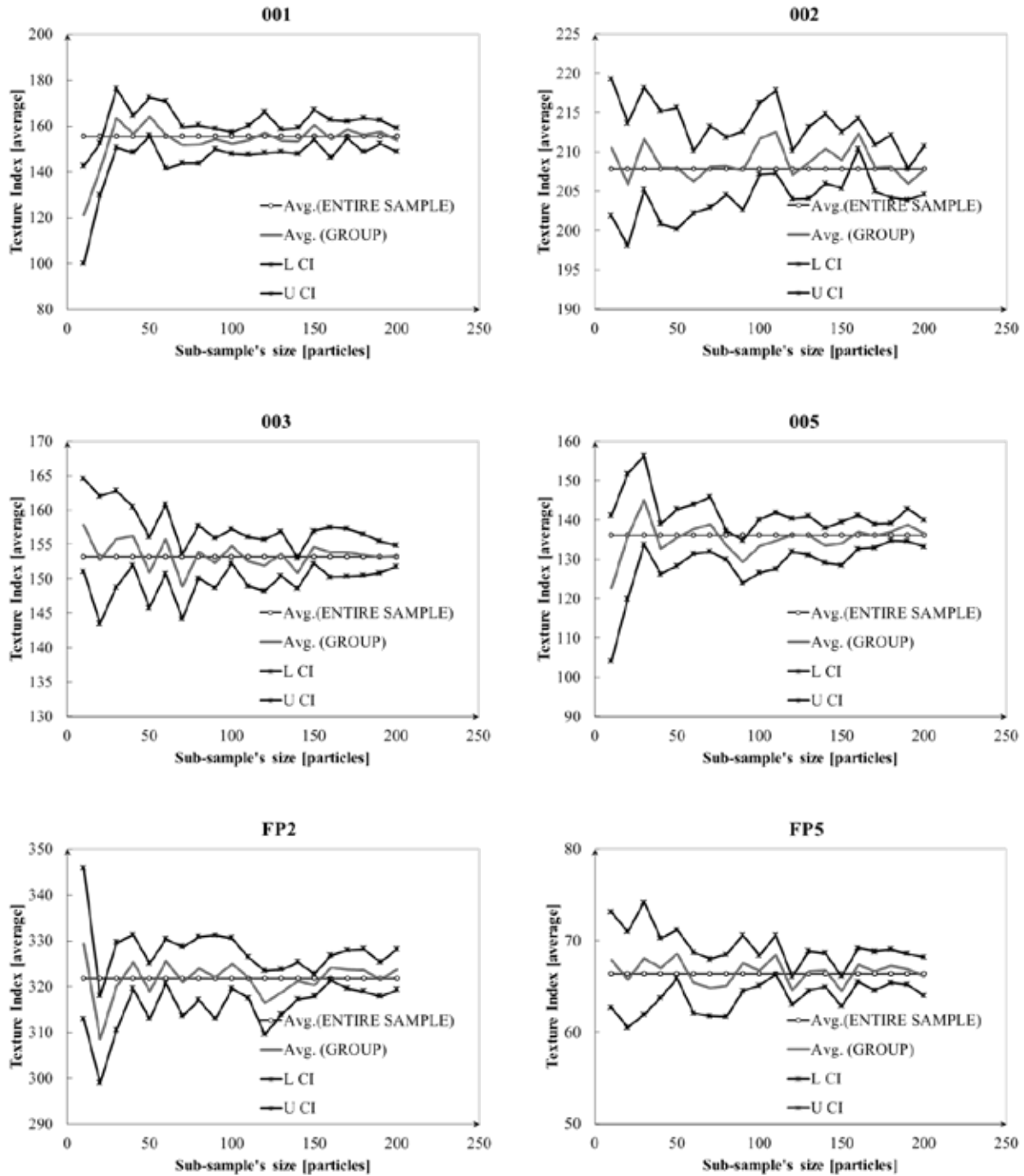
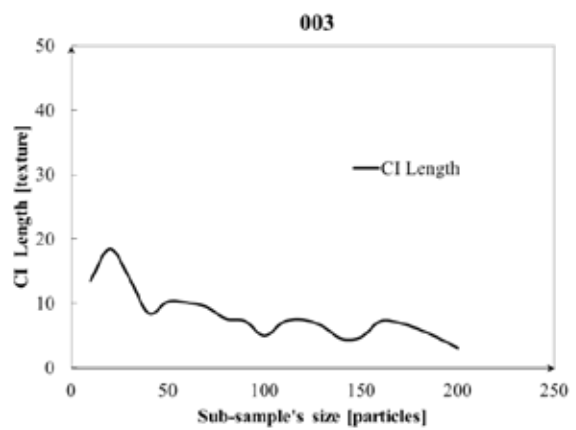
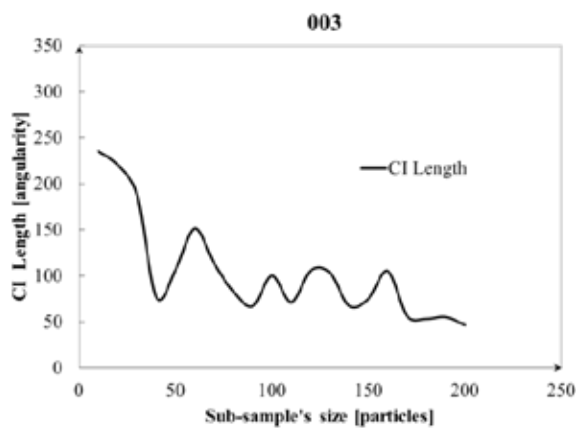
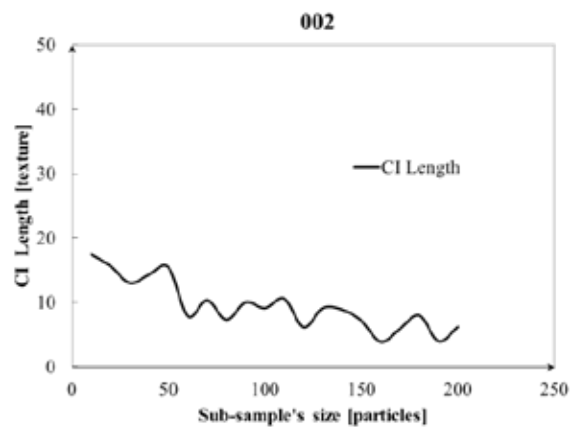
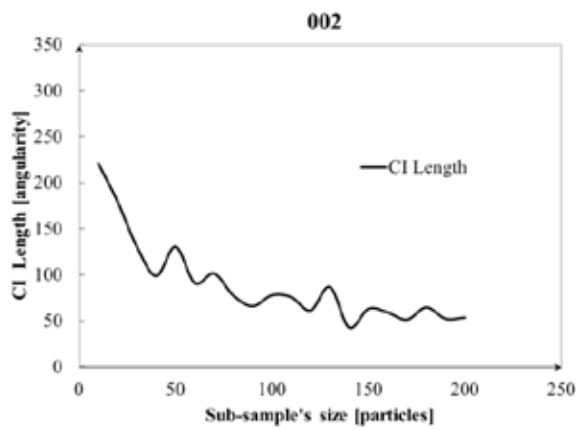
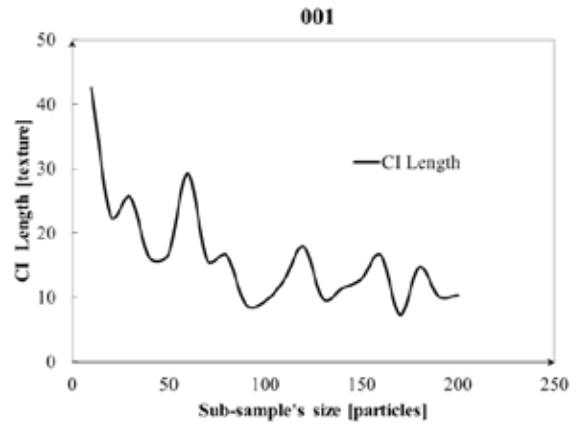
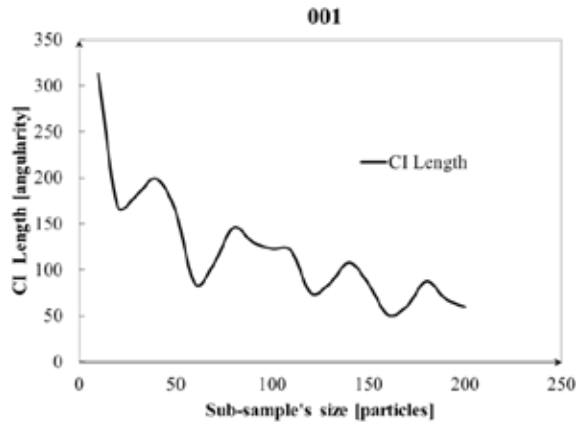


Figure 3.3. Average distributions of *texture* index.

Figure 3.2 clearly indicates that the angularity converges at around sub-sample size of 75. The texture, however, converged at around 100 particles as shown in Figure 3.3. Furthermore, Figure 3.4, which illustrates the length of the CI, shows that the CI lengths of both angularity and texture remain almost constant at around 100 particles.



(a)

(b)

Figure 3.4. Trends of CI lengths for different sub-sample sizes: (a) angularity data; (b) texture data.

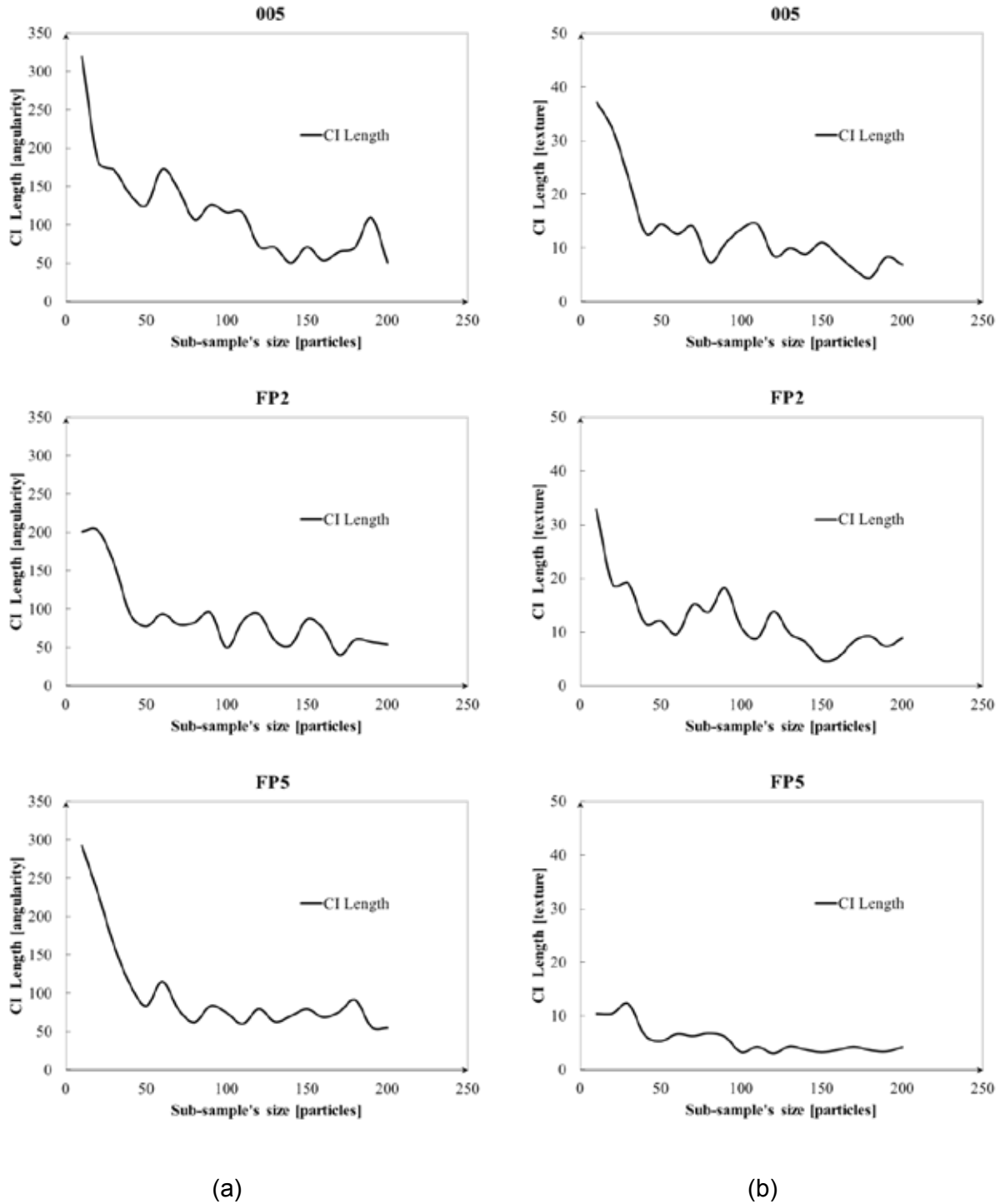


Figure 3.4. Trends of CI lengths for different sub-sample sizes: (a) angularity data; (b) texture data.

3.1.3 Asymptotic Analysis

To further investigate the minimum number of aggregate particles required for scanning with AIMS, an asymptotic analysis was conducted. In this analysis, the changes in shape properties (angularity and texture) were tracked as functions of the number of particles scanned. Figures 3.5 and 3.6 illustrate

angularity and texture analyses, respectively. It is clearly evident that the average of both angularity and texture reach a constant value at around 110 particles. Based on the sub-sample and asymptotic analyses, the research team decided that 120 particles would have to be scanned with AIMS.

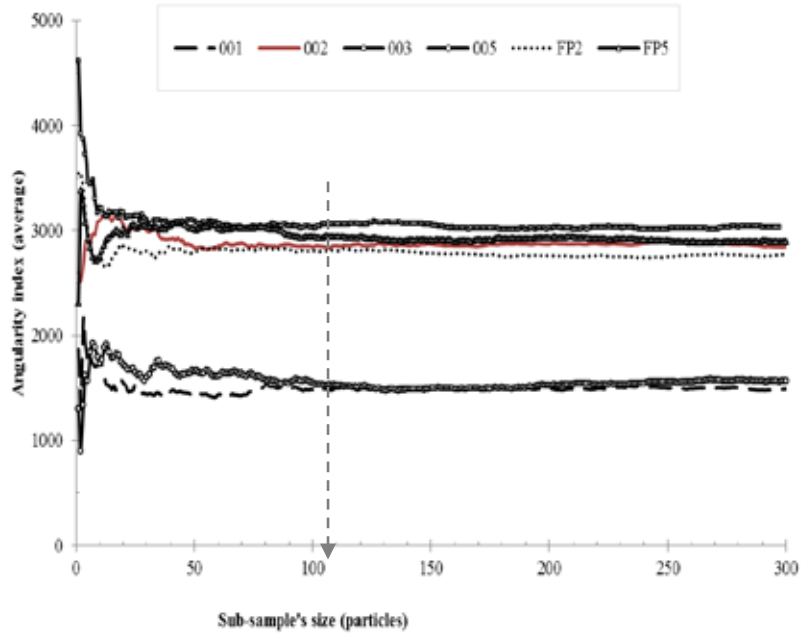


Figure 3.5. Asymptotic analysis for angularity.

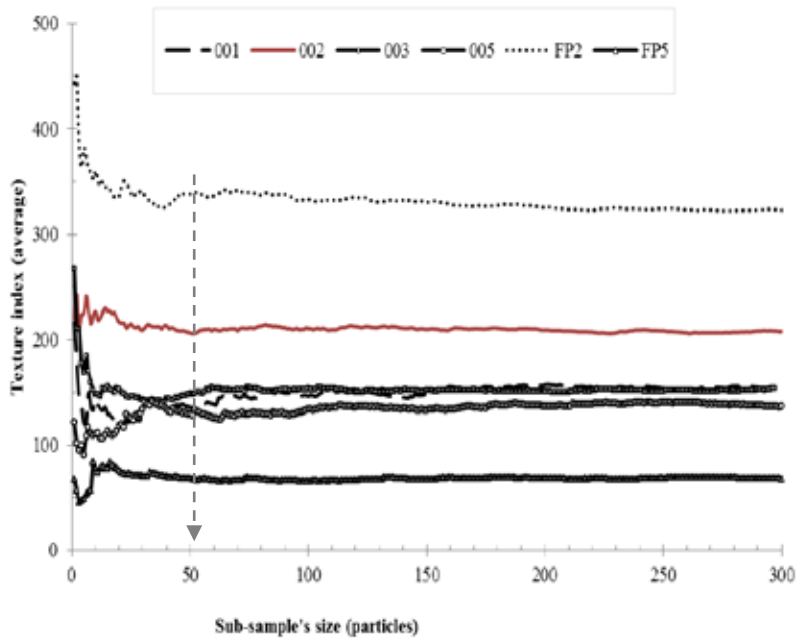


Figure 3.6. Asymptotic analysis for texture.

3.1.4 Manual Random Sampling

The sub-sample and asymptotic analyses were based on computer algorithms and were conducted by sampling from already scanned materials. Thus, it was necessary to check whether the 120 particles criterion would remain valid if the aggregate particles were manually sampled. Therefore, the same six sources selected in the previous analyses were used to study the effect of the manual (operator) selection of aggregate particles. Two testing approaches were considered:

The first approach, known as “combined” [C1-C3], consisted of the following steps:

1. 120 particles of the aggregate sample were randomly selected and scanned;
2. The scanned particles were returned to the sample bag and mixed with the rest of the material;
3. Steps 1-2 were repeated two more times.

The second approach, known as “separated” [S1-S3], consisted of the following steps:

1. 120 particles of the aggregate sample were randomly selected and scanned;
2. The scanned particles were kept apart, and another 120 aggregate particles were randomly selected and scanned;
3. Step 2 was repeated one more time.

The angularity results are summarized in Figure 3.7 and texture results are summarized in Figure 3.8. The two figures clearly indicate that both angularity and texture results were very close to the averages of the entire sample in all six cases, which further confirmed that the selection of 120 aggregate particles for scanning with AIMS was appropriate.

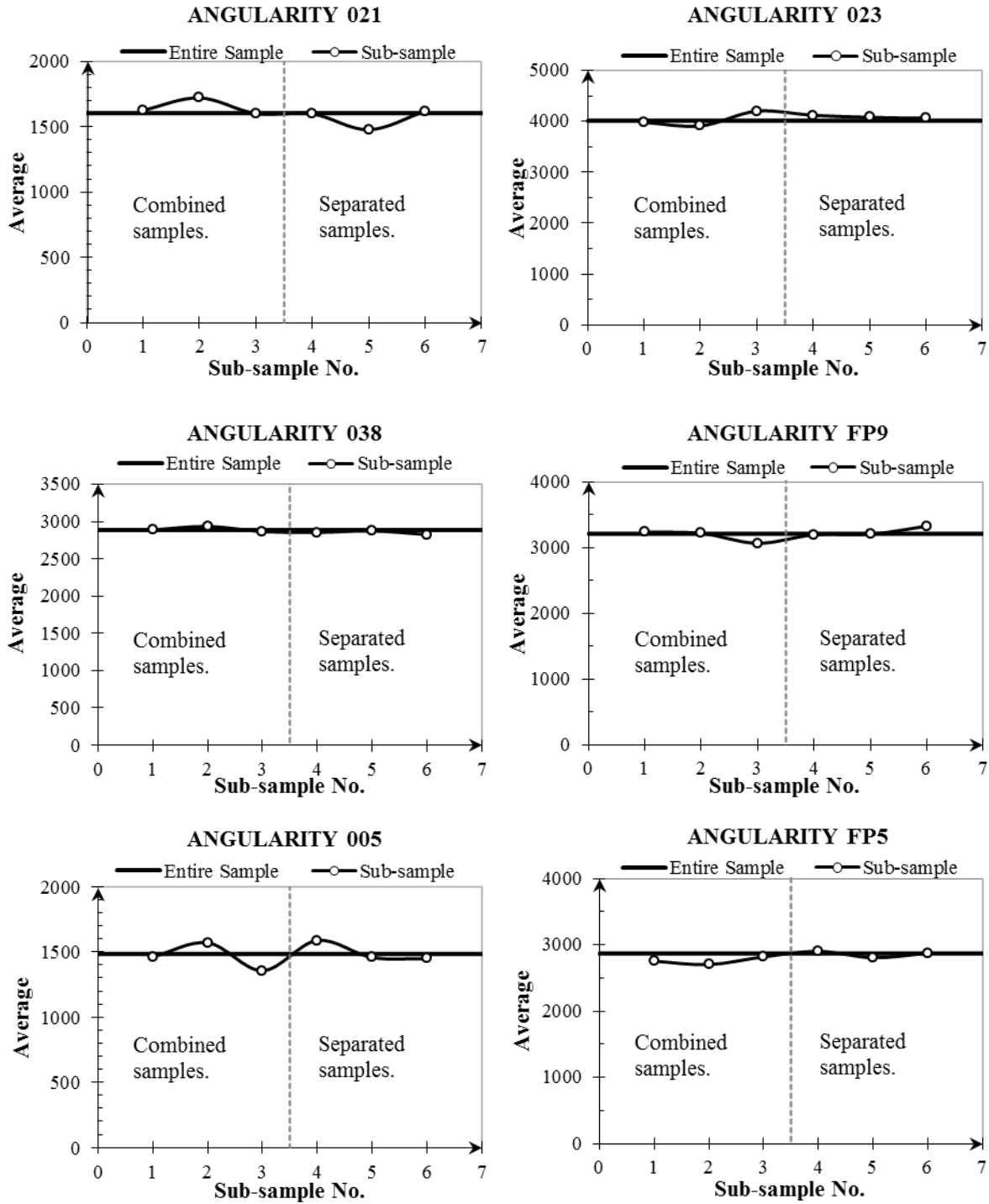


Figure 3.7. Manual random sampling (angularity).

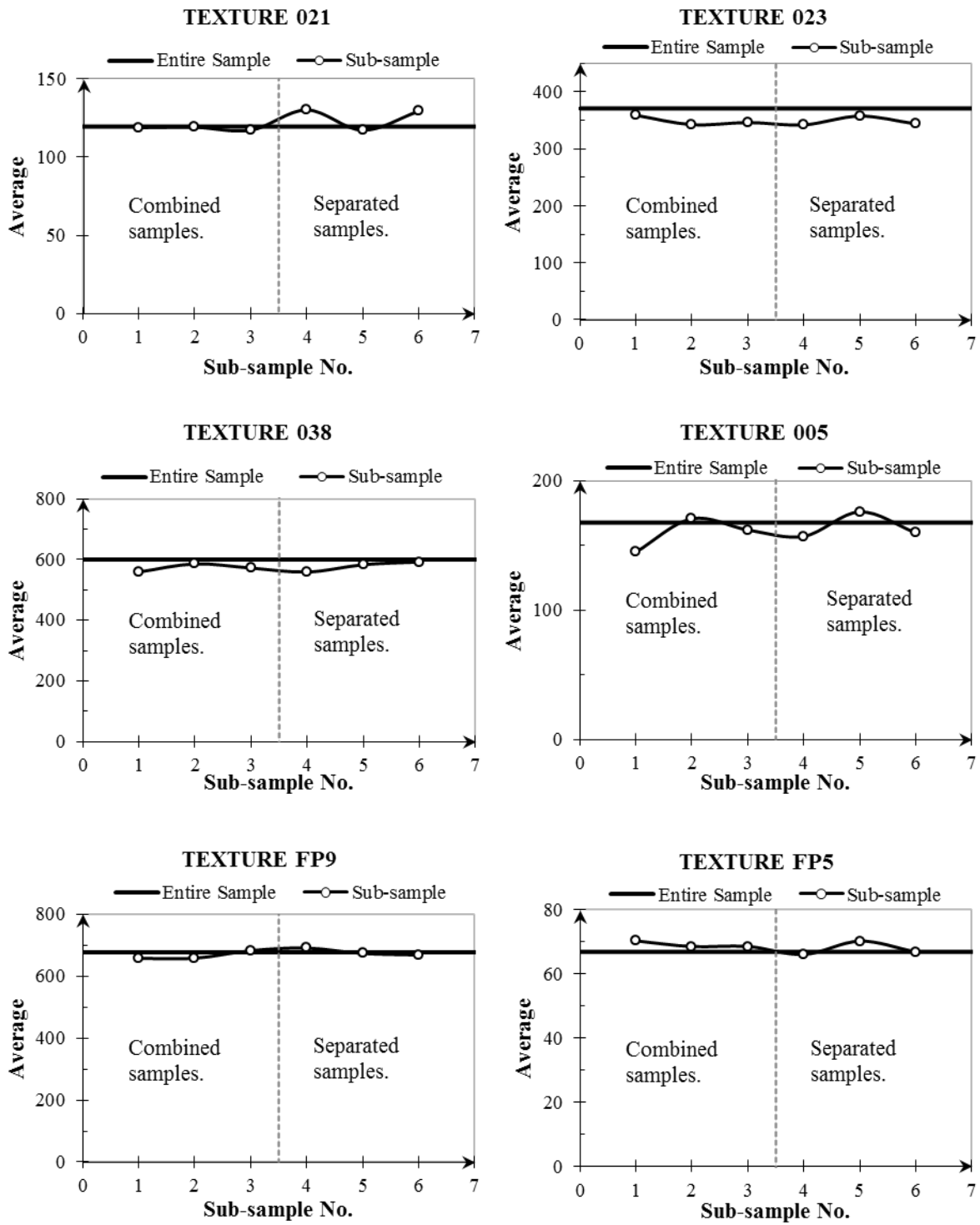


Figure 3.8. Manual random sampling (texture).

3.2 TERMINAL POLISHING

3.2.1 Stage 1: Preliminary Evaluation

In order to determine the polishing time required in Micro-Deval to reach terminal polishing, aggregate samples from the eleven sources in Table 2.1 were polished in the Micro-Deval at different time intervals: 0, 15, 30, 45, 60, 75, 90, 105, and 180 minutes. After each time interval, both AIMS and E-UIAIA were used to measure aggregate texture for the particles retained in the 3/8 in. sieve. The texture average and standard deviation of the tested samples are presented in Table 3.3.

Table 3.3 Texture Index Average and Standard Deviation by AIMS

IDOT Sample	Texture Index	Time in the Micro-Deval [min]								
		0	15	30	45	60	75	90	105	180
FP1	Average	266.3	201.0	176.8	164.3	153.0	147.7	133.2	138.0	121.1
	S. Dev.	91.0	62.8	57.9	60.5	60.4	50.9	51.9	53.5	51.4
FP2	Average	321.8	247.0	222.3	204.5	192.1	183.8	166.3	166.0	144.9
	S. Dev.	87.4	69.2	58.4	57.6	53.2	48.8	47.2	45.2	41.8
FP3	Average	189.2	144.8	128.8	126.0	104.6	106.8	98.8	95.5	90.8
	S. Dev.	67.0	55.7	42.6	54.4	38.2	39.9	34.1	32.9	30.4
FP4	Average	159.8	154.7	152.0	144.1	134.3	123.6	125.3	119.3	112.0
	S. Dev.	74.0	75.1	89.0	87.7	82.7	70.3	70.1	64.3	56.9
FP5	Average	67.1	64.0	60.9	55.0	52.0	52.0	57.1	54.3	55.3
	S. Dev.	38.3	40.0	36.8	27.1	22.0	23.4	31.0	25.7	28.0
FP6	Average	223.5	215.0	200.8	190.0	171.3	166.6	174.0	157.9	164.3
	S. Dev.	138.4	144.2	131.1	137.8	137.4	114.3	122.0	113.0	137.4
FP7	Average	154.3	193.6	193.8	200.7	217.3	204.3	201.8	202.7	209.5
	S. Dev.	84.7	104.6	99.7	94.7	107.7	105.1	101.8	98.5	98.2
FP8	Average	387.2	430.7	438.2	449.4	406.2	423.0	416.7	395.0	400.0
	S. Dev.	107.0	87.6	101.4	113.9	97.9	107.4	109.7	119.7	110.9
FP10	Average	613.1	546.0	512.4	520.0	492.1	496.7	462.8	475.4	437.9
	S. Dev.	194.6	186.7	174.5	151.7	156.3	145.4	169.6	153.8	134.1
FP11	Average	337.5	367.7	354.2	360.2	351.7	345.6	333.0	352.3	337.6
	S. Dev.	107.2	110.3	109.2	97.7	102.8	94.7	103.9	104.7	98.3

In order to evaluate the efficacy of the current procedure to reach terminal texture at 180 minutes, a t-test statistical analysis was conducted to compare aggregate texture between consecutive Micro-Deval polishing time intervals. A 95% Confidence Interval (CI) was calculated for the difference in the texture mean between consecutive Micro-Deval time intervals. The CIs are obtained using the following equation:

$$Z_0 = \bar{X}_1 - \bar{X}_2 - Z_{\alpha/2} \sqrt{\frac{\sigma_1^2}{n_1} + \frac{\sigma_2^2}{n_2}} \leq \mu_1 - \mu_2 \leq Z_0 = \bar{X}_1 - \bar{X}_2 + Z_{\alpha/2} \sqrt{\frac{\sigma_1^2}{n_1} + \frac{\sigma_2^2}{n_2}} \quad (1)$$

where $Z_{\alpha/2}$ is the upper $\alpha/2$ percentage point of the standard normal distribution ($\alpha = 0.05$ for this study).

Table 3.4 lists the CIs for the eleven samples. The results of this analysis are illustrated in Figure 3.9 by the CI lower limit (L-CI) and CI upper limit (U-CI) lines. For example, the L-CI and U-CI points at 180 minutes are the CI limits for the difference in the texture mean between 105 and 180 minutes samples. A CI containing zero indicates that the texture averages are not different, which indicates that 105 minutes is sufficient polishing time if the CI at 180 contains zero. The CI-lines in Figure 3.9 indicate that not all the CIs at 180 minutes contain zero. The presence of significant remaining surface texture is shown by the values of confidence intervals that do not contain zero: FP1, FP2, FP9 and FP10. Consequently, it was decided to extend the polishing time to achieve terminal texture. However, in order to subject the samples to a polishing time that would produce terminal texture, a preliminary estimate of such value was required. This was achieved by fitting an analytical model describing the behavior of aggregate texture after several polishing times through the Micro-Deval:

$$\text{Texture}(t) = a + b * e^{-c*t} \quad (2)$$

where texture(t) is the aggregate texture as function of time, t, in minutes; a and b are regression model parameters representing initial and final texture; and c is a parameter that represents the rate of texture loss. The texture values at 0, 15, 30 ... and 180 minutes were fitted to the analytical model (Eq. 2). The least squares method was used to obtain parameters a, b, and c that best fit the data points as shown in Figure 3.9. The fitting parameters are summarized in Table 3.5.

Table 3.4 Statistical Inference on the Texture Means

IDOT Sample	Time Micro-Deval [min]	No. Particles	Texture Average	Std. Dev.	Lower CI	Upper CI
FP1	0	338	266.3	91.0		
	15	333	201.0	62.8	53.54	77.16
	30	309	176.8	57.9	14.78	33.46
	45	286	164.3	60.5	3.03	22.10
	60	274	153.1	60.4	1.19	21.22
	75	265	147.7	50.9	-4.01	14.82
	90	243	133.2	51.9	5.53	23.43
	105	225	138.0	48.9	-13.96	4.30
	180	184	121.2	51.4	7.07	26.65
FP2	0	353	321.8	87.4		
	15	318	247.0	69.2	62.90	86.66
	30	292	222.3	58.4	14.54	34.82
	45	310	204.5	57.6	8.55	27.10
	60	263	192.1	53.2	3.32	21.50
	75	279	183.8	48.8	-0.33	16.90
	90	229	166.3	47.2	9.12	25.88
	105	246	166.0	45.2	-7.98	8.67
	180	195	144.9	41.8	12.87	29.15
FP3	0	317	189.2	67.0		
	15	323	144.8	55.7	34.86	53.97
	30	285	128.8	42.6	8.16	23.83
	45	253	126.0	54.4	-5.51	11.15
	60	236	104.6	38.2	13.13	29.70
	75	218	106.8	39.9	-9.43	4.97
	90	217	98.8	34.1	1.06	15.00

IDOT Sample	Time Micro-Deval [min]	No. Particles	Texture Average	Std. Dev.	Lower CI	Upper CI
	105	196	95.5	32.9	-3.19	9.72
	180	173	90.8	30.4	-1.74	11.18
FP4	0	320	159.8	74.0		
	15	351	154.7	75.0	-6.20	16.37
	30	314	152.0	89.0	-9.83	15.36
	45	315	144.1	87.7	-5.92	21.71
	60	288	134.3	82.7	-3.88	23.34
	75	263	123.6	70.3	-2.10	23.48
	90	264	125.3	70.1	-13.64	10.34
	105	262	119.3	64.3	-5.48	17.51
	180	227	112.0	56.9	-3.46	18.03
	FP5	0	492	67.1	38.3	
15		388	64.0	40.0	-2.17	8.28
30		304	60.9	36.8	-2.58	8.89
45		238	55.0	27.1	0.47	11.22
60		180	52.0	22.0	-1.61	7.79
75		135	52.0	23.4	-5.11	5.06
90		135	57.1	31.1	-11.66	1.46
105		107	54.3	25.7	-4.32	9.98
180		49	55.3	28.0	-10.23	8.21
FP6	0	469	223.5	138.4		
	15	363	215.0	144.2	-10.93	27.90
	30	240	200.8	131.1	-8.01	36.50
	45	222	190.0	137.8	-13.82	35.34
	60	189	171.3	137.4	-7.93	45.46
	75	205	166.6	114.3	-20.41	29.73
	90	186	174.0	122.0	-30.94	16.05
	105	161	157.9	113.0	-8.58	40.91
	180	110	164.3	137.4	-37.42	24.66
FP7	0	378	154.3	84.7		
	15	378	193.6	104.6	-52.89	-25.75
	30	375	193.8	99.7	-14.80	14.39
	45	372	200.7	94.7	-20.82	7.06
	60	378	217.3	107.7	-31.14	-2.12
	75	366	204.3	105.1	-2.26	28.32
	90	360	201.8	101.8	-12.54	17.56
	105	368	202.7	98.5	-15.47	13.65
	180	352	209.5	98.2	-21.16	7.57
FP8	0	248	387.2	107.0		
	15	249	430.7	87.6	-60.72	-26.32
	30	254	438.2	101.4	-24.05	9.06
	45	241	449.4	113.9	-30.24	7.82
	60	246	406.2	97.9	24.39	62.15
	75	236	423.0	107.4	-35.18	1.57
	90	217	416.7	109.7	-13.71	26.32
	105	234	395.0	119.7	0.46	42.80
	180	211	400.0	110.9	-26.43	16.44

IDOT Sample	Time Micro-Deval [min]	No. Particles	Texture Average	Std. Dev.	Lower CI	Upper CI
FP9	0	423	688.3	162.3		
	30	304	693.7	176.6	-30.58	19.76
	75	218	689.4	176.8	-26.44	35.04
	105	186	682.8	185.7	-28.96	42.11
	180	131	612.6	198.6	26.97	113.42
FP10	0	387	613.1	194.6		
	15	366	546.0	186.7	39.80	94.27
	30	341	512.4	174.5	7.01	60.26
	45	341	520.0	151.7	-32.17	16.91
	60	324	492.1	156.3	4.55	51.40
	75	333	496.7	145.4	-27.75	18.44
	90	331	462.8	169.6	9.87	57.94
	105	310	475.4	153.7	-37.62	12.44
FP11	180	296	437.9	134.1	14.60	60.48
	0	389	337.5	107.2		
	15	315	367.7	110.3	-46.37	-14.01
	30	271	354.2	109.2	-4.28	31.36
	45	248	360.2	97.7	-23.77	11.83
	60	225	351.7	102.8	-9.69	26.54
	75	205	345.5	94.7	-12.39	24.94
	90	176	333.0	103.9	-7.62	32.56
	105	159	352.3	104.7	-41.70	3.05
180	127	337.6	98.3	-8.86	38.34	

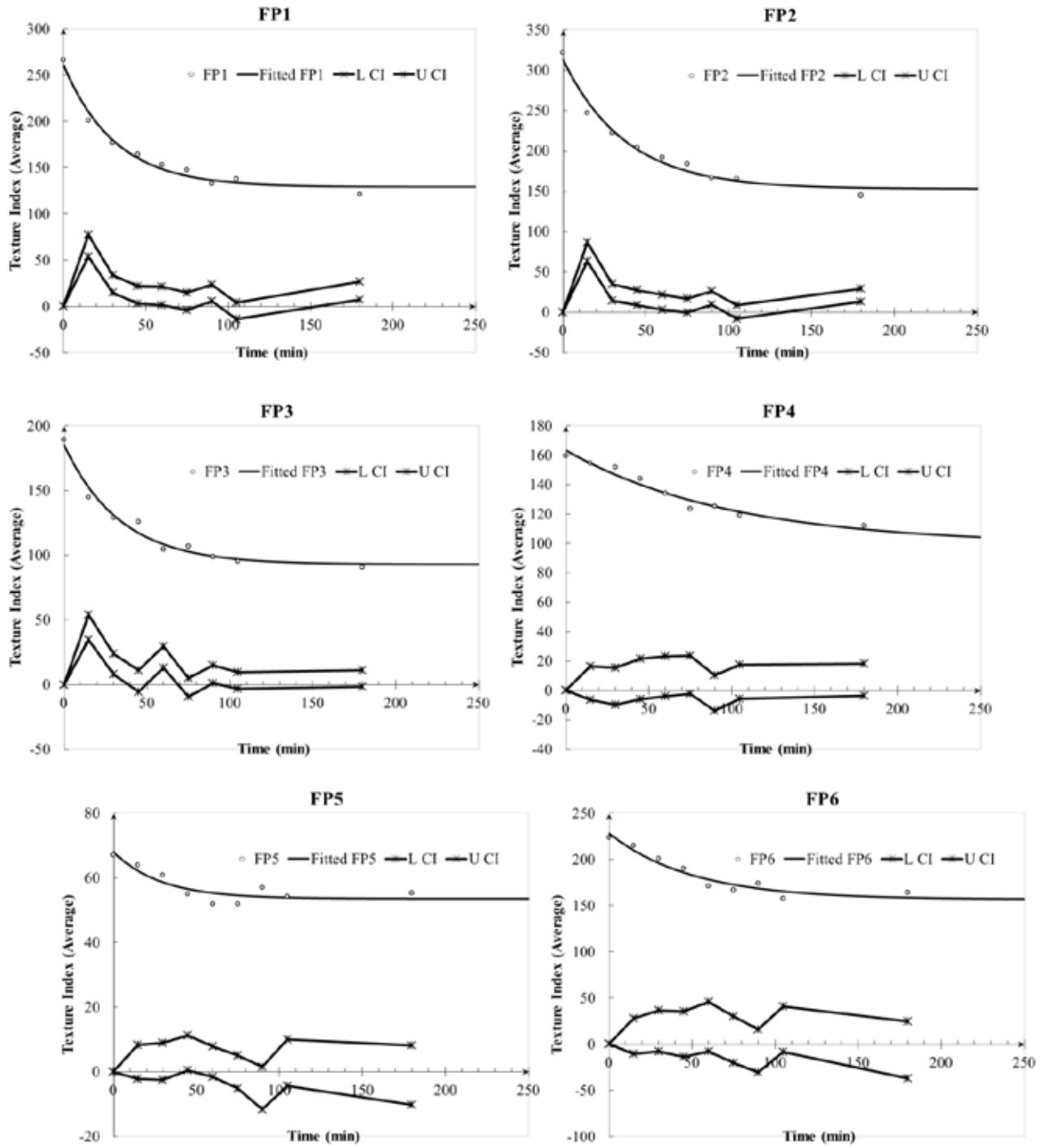


Figure 3.9 Averages of texture index, fitted curves, and confidence intervals [Stage 1].

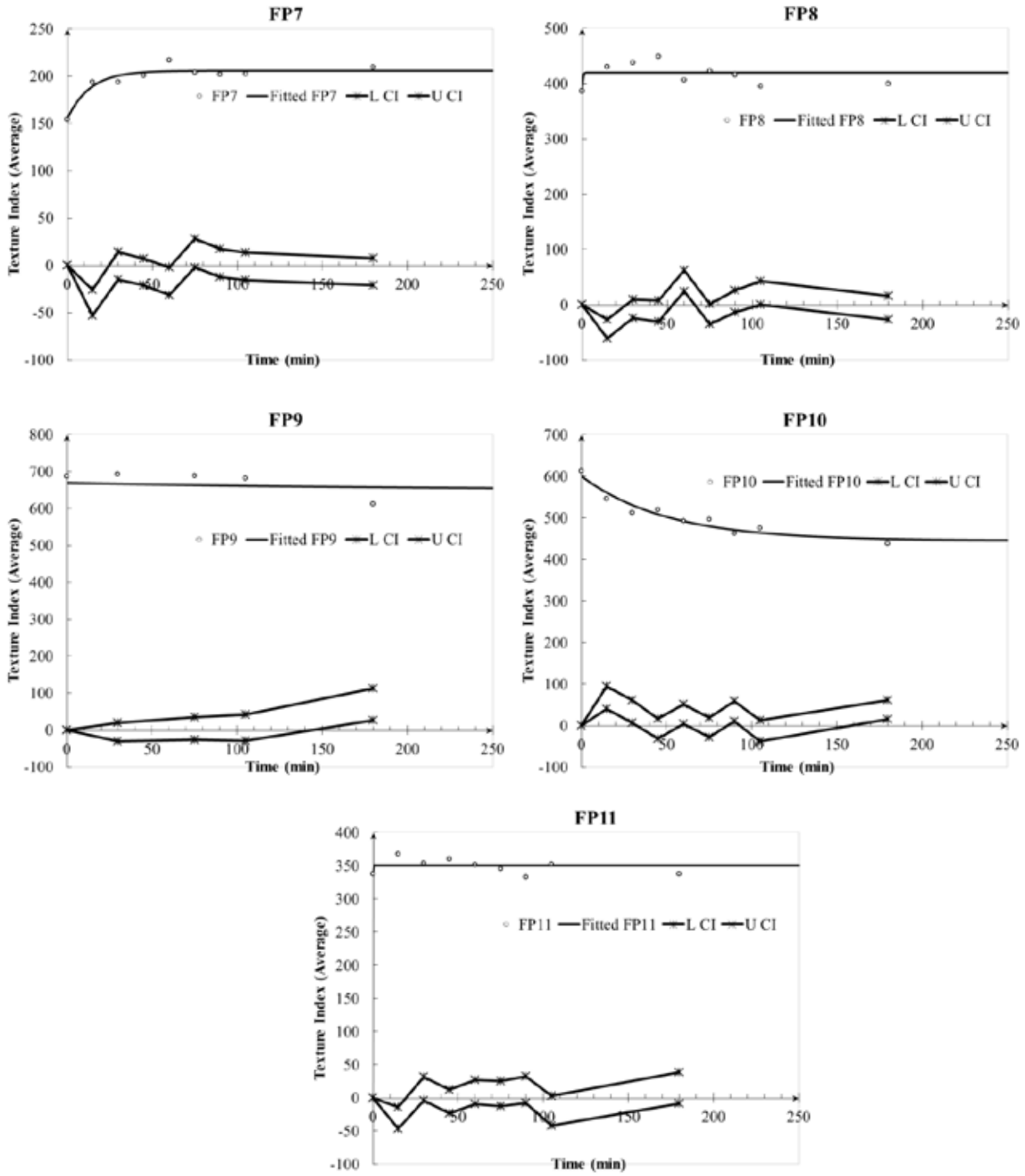


Figure 3.9 Averages of texture index, fitted curves, and confidence intervals [Stage 1].

Table 3.5 Function Fitting Results

IDOT Sample	Equation	Fitting Parameters			Goodness of fit
		a	b	c	R ²
FP1	$Texture(t) = a + b * e^{-c*t}$	129.20	131.90	3.21E-02	0.98
FP2		152.80	161.20	2.65E-02	0.98
FP3		92.88	92.76	2.97E-02	0.98
FP4		99.05	64.43	1.00E-02	0.96
FP5		53.54	14.59	3.51E-02	0.82
FP6		156.60	71.76	2.00E-02	0.93
FP7		205.90	-51.00	7.57E-02	0.90
FP8		419.90	-32.70	2.31E+00	0.27
FP9		649.90	20.06	5.03E-03	0.10
FP10		444.80	155.70	1.99E-02	0.93
FP11		350.30	-12.77	5.99E+02	0.14

The next section describes how the polishing data (up to 180 minutes) were used to estimate the required final polishing time.

3.2.2 Stage 2: Extended Polishing Time

The fitted polishing curves in Stage 1 were used to estimate the aggregate texture for extended polishing times in the range of 195 to 270 minutes at 15 minute increments. Assuming the variance for the extended polishing times is equal to the variance at 180 minutes, the CIs were calculated at the extended polishing times for each aggregate source. The t-test results are presented graphically in Figure 3.10 and numerically in Table 3.6. Close examination of these results indicated that all aggregate materials tested would reach terminal texture within 210 minutes of polishing. Therefore, each sample was subjected to a final polishing time of 210 minutes in the next stage of this analysis.

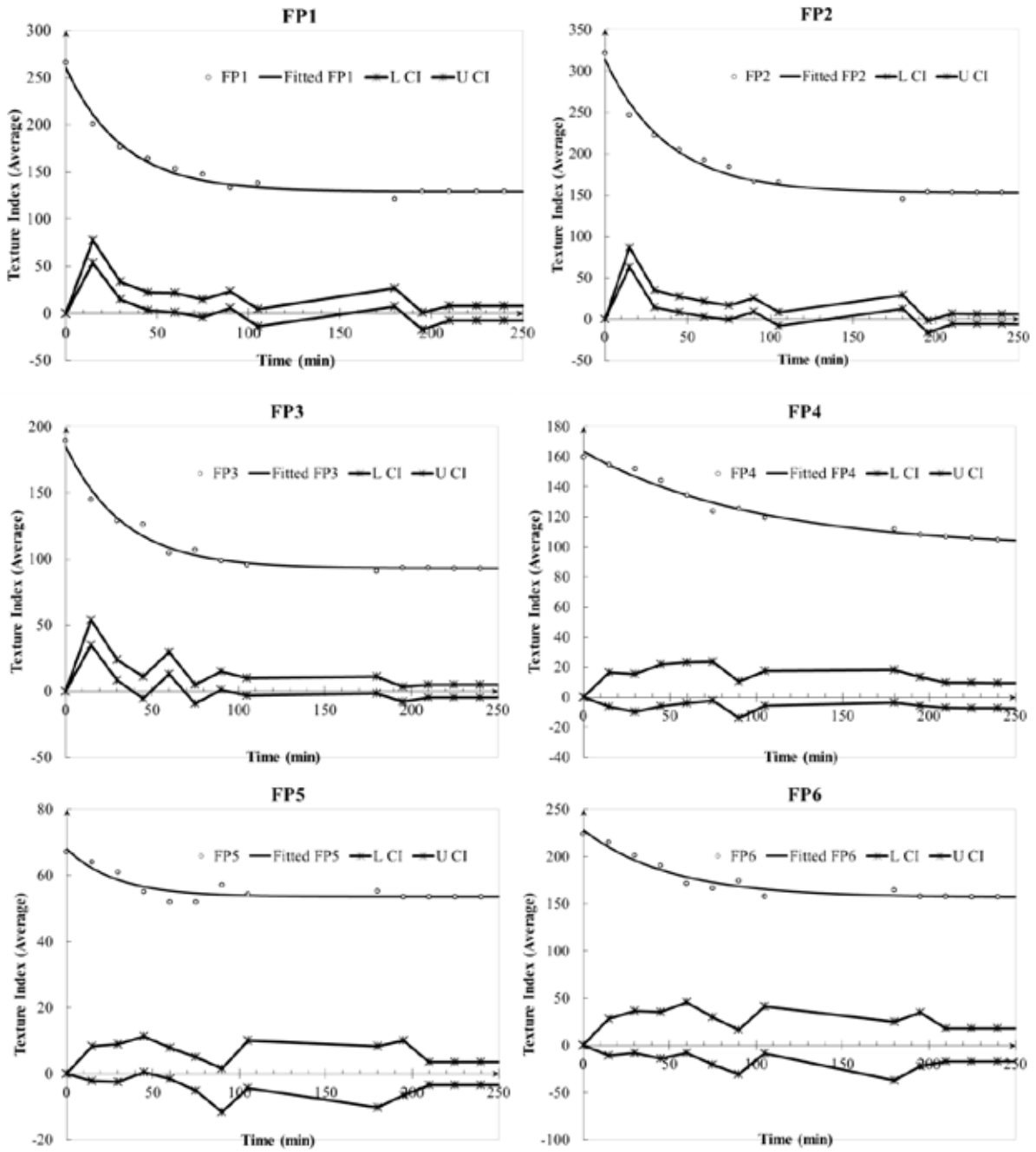


Figure 3.10 Averages of texture index, fitted curves, and confidence intervals [Stage 2].

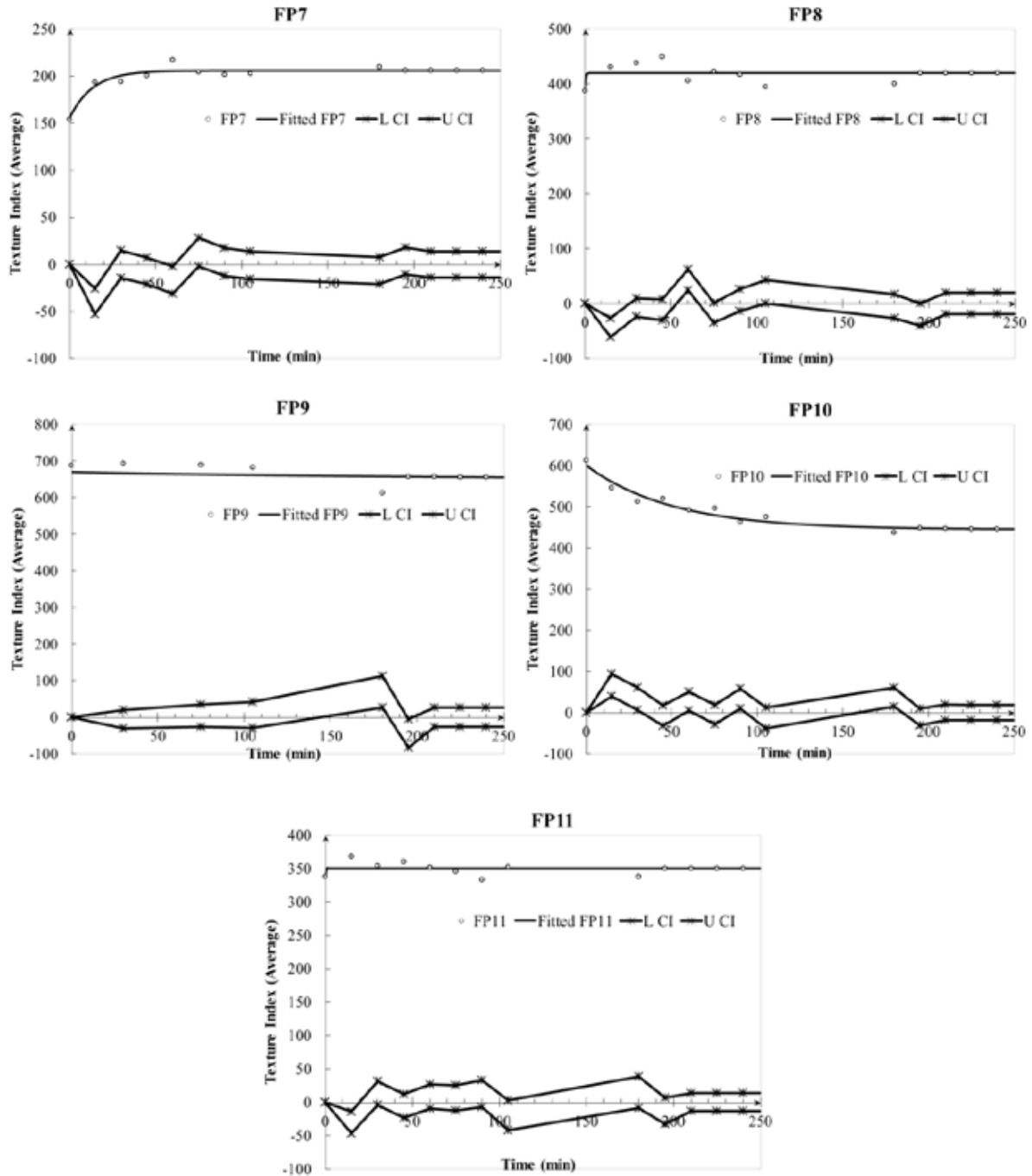


Figure 3.10 Averages of texture index, fitted curves, and confidence intervals [Stage 2].

Table 3.6 Statistical Inference on the Texture Means

IDOT Sample	Time Micro-Deval [min]	No. Particles	Texture Average	Std. Dev.	Lower CI	Upper CI
FP1	0	338	266.31	90.96		
	15	333	200.96	62.84	53.54	77.16
	30	309	176.84	57.91	14.78	33.46
	45	286	164.27	60.52	3.03	22.10
	60	274	153.07	60.38	1.19	21.22
	75	265	147.67	50.92	-4.01	14.82
	90	243	133.19	51.87	5.53	23.43
	105	225	138.02	48.87	-13.96	4.30
	180	184	121.15	51.36	7.07	26.65
	195	338	129.45	51.36	-17.52	0.92
	210	338	129.36	51.36	-7.65	7.84
	225	338	129.30	51.36	-7.68	7.80
	240	338	129.26	51.36	-7.71	7.78
	255	338	129.24	51.36	-7.72	7.77
270	338	129.22	51.36	-7.73	7.76	
FP2	0	353	321.77	87.42		
	15	318	246.99	69.24	62.90	86.66
	30	292	222.31	58.39	14.54	34.82
	45	310	204.49	57.64	8.55	27.10
	60	263	192.08	53.24	3.32	21.50
	75	279	183.80	48.82	-0.33	16.90
	90	229	166.29	47.21	9.12	25.88
	105	246	165.95	45.24	-7.98	8.67
	180	195	144.94	41.77	12.87	29.15
	195	353	153.73	41.77	-16.09	-1.48
	210	353	153.42	41.77	-5.86	6.47
	225	353	153.22	41.77	-5.96	6.37
	240	353	153.08	41.77	-6.02	6.30
	255	353	152.99	41.77	-6.07	6.25
270	353	152.93	41.77	-6.10	6.22	
FP3	0	317	189.23	67.01		
	15	323	144.81	55.68	34.86	53.97
	30	285	128.82	42.64	8.16	23.83
	45	253	125.99	54.37	-5.51	11.15
	60	236	104.57	38.21	13.13	29.70
	75	218	106.80	39.89	-9.43	4.97
	90	217	98.77	34.07	1.06	15.00
	105	196	95.51	32.86	-3.19	9.72
	180	173	90.79	30.44	-1.74	11.18
	195	323	93.16	30.44	-7.99	3.25
	210	323	93.06	30.44	-4.59	4.80
	225	323	93.00	30.44	-4.63	4.76
	240	323	92.95	30.44	-4.65	4.74
	255	323	92.93	30.44	-4.67	4.72
270	323	92.91	30.44	-4.68	4.71	
FP4	0	320	159.80	73.96		

IDOT Sample	Time Micro-Deval [min]	No. Particles	Texture Average	Std. Dev.	Lower CI	Upper CI
	15	351	154.72	75.05	-6.20	16.37
	30	314	151.95	89.03	-9.83	15.36
	45	315	144.06	87.73	-5.92	21.71
	60	288	134.33	82.75	-3.88	23.34
	75	263	123.64	70.34	-2.10	23.48
	90	264	125.29	70.06	-13.64	10.34
	105	262	119.28	64.34	-5.48	17.51
	180	227	111.99	56.87	-3.46	18.03
	195	352	108.18	56.87	-5.68	13.30
	210	352	106.91	56.87	-7.13	9.68
	225	352	105.81	56.87	-7.30	9.50
	240	352	104.87	56.87	-7.46	9.34
	255	352	104.06	56.87	-7.59	9.21
	270	352	103.36	56.87	-7.70	9.10
	0	492	67.10	38.33		
	15	388	64.04	40.00	-2.17	8.28
	30	304	60.89	36.75	-2.58	8.89
	45	238	55.04	27.05	0.47	11.22
	60	180	51.96	21.96	-1.61	7.79
	75	135	51.98	23.39	-5.11	5.06
	90	135	57.09	31.07	-11.66	1.46
FP5	105	107	54.26	25.65	-4.32	9.98
	180	49	55.27	28.00	-10.23	8.21
	195	500	53.56	28.00	-6.50	9.93
	210	500	53.55	28.00	-3.46	3.48
	225	500	53.55	28.00	-3.47	3.47
	240	500	53.54	28.00	-3.47	3.47
	255	500	53.54	28.00	-3.47	3.47
	270	500	53.54	28.00	-3.47	3.47
	0	469	223.52	138.37		
	15	363	215.04	144.22	-10.93	27.90
	30	240	200.79	131.14	-8.01	36.50
	45	222	190.03	137.84	-13.82	35.34
	60	189	171.27	137.39	-7.93	45.46
	75	205	166.60	114.29	-20.41	29.73
	90	186	174.05	122.01	-30.94	16.05
FP6	105	161	157.88	113.00	-8.58	40.91
	180	110	164.26	137.35	-37.42	24.66
	195	474	158.05	137.35	-22.28	34.70
	210	474	157.68	137.35	-17.11	17.86
	225	474	157.40	137.35	-17.21	17.77
	240	474	157.19	137.35	-17.28	17.69
	255	474	157.04	137.35	-17.33	17.64
	270	474	156.92	137.35	-17.37	17.60
	0	378	154.31	84.72		
FP7	15	378	193.63	104.61	-52.89	-25.75
	30	375	193.83	99.71	-14.80	14.39
	45	372	200.71	94.67	-20.82	7.06

IDOT Sample	Time Micro-Deval [min]	No. Particles	Texture Average	Std. Dev.	Lower CI	Upper CI
	60	378	217.33	107.74	-31.14	-2.12
	75	366	204.30	105.06	-2.26	28.32
	90	360	201.80	101.81	-12.54	17.56
	105	368	202.70	98.51	-15.47	13.65
	180	352	209.50	98.15	-21.16	7.57
	195	388	205.90	98.15	-10.56	17.76
	210	388	205.90	98.15	-13.81	13.81
	225	388	205.90	98.15	-13.81	13.81
	240	388	205.90	98.15	-13.81	13.81
	255	388	205.90	98.15	-13.81	13.81
	270	388	205.90	98.15	-13.81	13.81
	0	248	387.21	107.04		
	15	249	430.73	87.61	-60.72	-26.32
	30	254	438.23	101.43	-24.05	9.06
	45	241	449.44	113.88	-30.24	7.82
	60	246	406.16	97.93	24.39	62.15
	75	236	422.97	107.42	-35.18	1.57
	90	217	416.66	109.65	-13.71	26.32
FP8	105	234	395.03	119.71	0.46	42.80
	180	211	400.02	110.94	-26.43	16.44
	195	254	419.90	110.94	-40.13	0.38
	210	254	419.90	110.94	-19.29	19.29
	225	254	419.90	110.94	-19.29	19.29
	240	254	419.90	110.94	-19.29	19.29
	255	254	419.90	110.94	-19.29	19.29
	270	254	419.90	110.94	-19.29	19.29
	0	423	688.27	162.32		
	30	304	693.68	176.62	-30.58	19.76
	75	218	689.38	176.81	-26.44	35.04
	105	186	682.80	185.67	-28.96	42.11
	180	131	612.60	198.61	26.97	113.42
FP9	195	423	657.43	198.61	-83.75	-5.90
	210	423	656.88	198.61	-26.22	27.31
	225	423	656.37	198.61	-26.26	27.27
	240	423	655.90	198.61	-26.30	27.24
	255	423	655.47	198.61	-26.33	27.20
	270	423	655.06	198.61	-26.36	27.17
	0	387	613.08	194.62		
	15	366	546.04	186.71	39.80	94.27
	30	341	512.41	174.50	7.01	60.26
	45	341	520.04	151.66	-32.17	16.91
	60	324	492.06	156.27	4.55	51.40
	75	333	496.72	145.40	-27.75	18.44
	90	331	462.82	169.56	9.87	57.94
	105	310	475.41	153.75	-37.62	12.44
	180	296	437.87	134.08	14.60	60.48
	195	400	448.05	134.08	-30.32	9.98

IDOT Sample	Time Micro-Deval [min]	No. Particles	Texture Average	Std. Dev.	Lower CI	Upper CI
FP11	210	400	447.21	134.08	-17.75	19.42
	225	400	446.59	134.08	-17.96	19.20
	240	400	446.13	134.08	-18.12	19.04
	255	400	445.79	134.08	-18.24	18.92
	270	400	445.53	134.08	-18.33	18.84
	0	389	337.54	107.16		
	15	315	367.73	110.28	-46.37	-14.01
	30	271	354.19	109.23	-4.28	31.36
	45	248	360.16	97.67	-23.77	11.83
	60	225	351.73	102.79	-9.69	26.54
	75	205	345.46	94.68	-12.39	24.94
	90	176	332.99	103.91	-7.62	32.56
	105	159	352.32	104.73	-41.70	3.05
	180	127	337.58	98.28	-8.86	38.34
	195	389	350.30	98.28	-32.41	6.96
	210	389	350.30	98.28	-13.81	13.81
	225	389	350.30	98.28	-13.81	13.81
	240	389	350.30	98.28	-13.81	13.81
	255	389	350.30	98.28	-13.81	13.81
	270	389	350.30	98.28	-13.81	13.81

3.2.3 Stage 3: Terminal Polishing

In this stage, an additional sample from each source was subjected to a Micro-Deval polishing time of 210 minutes. Table 3.7 presents the fitting parameters for the 210 minutes polishing curves. Figure 3.11 shows the fitting curves and CI analyses, which indicate that nine sources reached terminal texture and that only FP1 and FP11 CIs did not include zero at 210 minutes. Table 3.8 summarizes the CIs numerically.

Table 3.7 Function Fitting Results

IDOT Sample	Equation	Fitting Parameters			Goodness of Fit
		a	b	c	R ²
FP1	$Texture(t) = a + b * e^{-c*t}$	120.80	137.60	0.0266	0.97
FP2		151.10	162.10	0.0256	0.98
FP3		93.27	92.70	0.0304	0.98
FP4		97.16	65.95	0.0095	0.97
FP5		53.34	14.83	0.0341	0.83
FP6		164.70	64.50	0.0256	0.88
FP7		204.10	-49.39	0.0866	0.86
FP8		437.70	-16.49	-0.0030	0.06
FP9		659.10	29.18	0.9935	0.10
FP10		436.80	161.80	0.0176	0.94
FP11		353.80	-16.31	2.4130	0.12

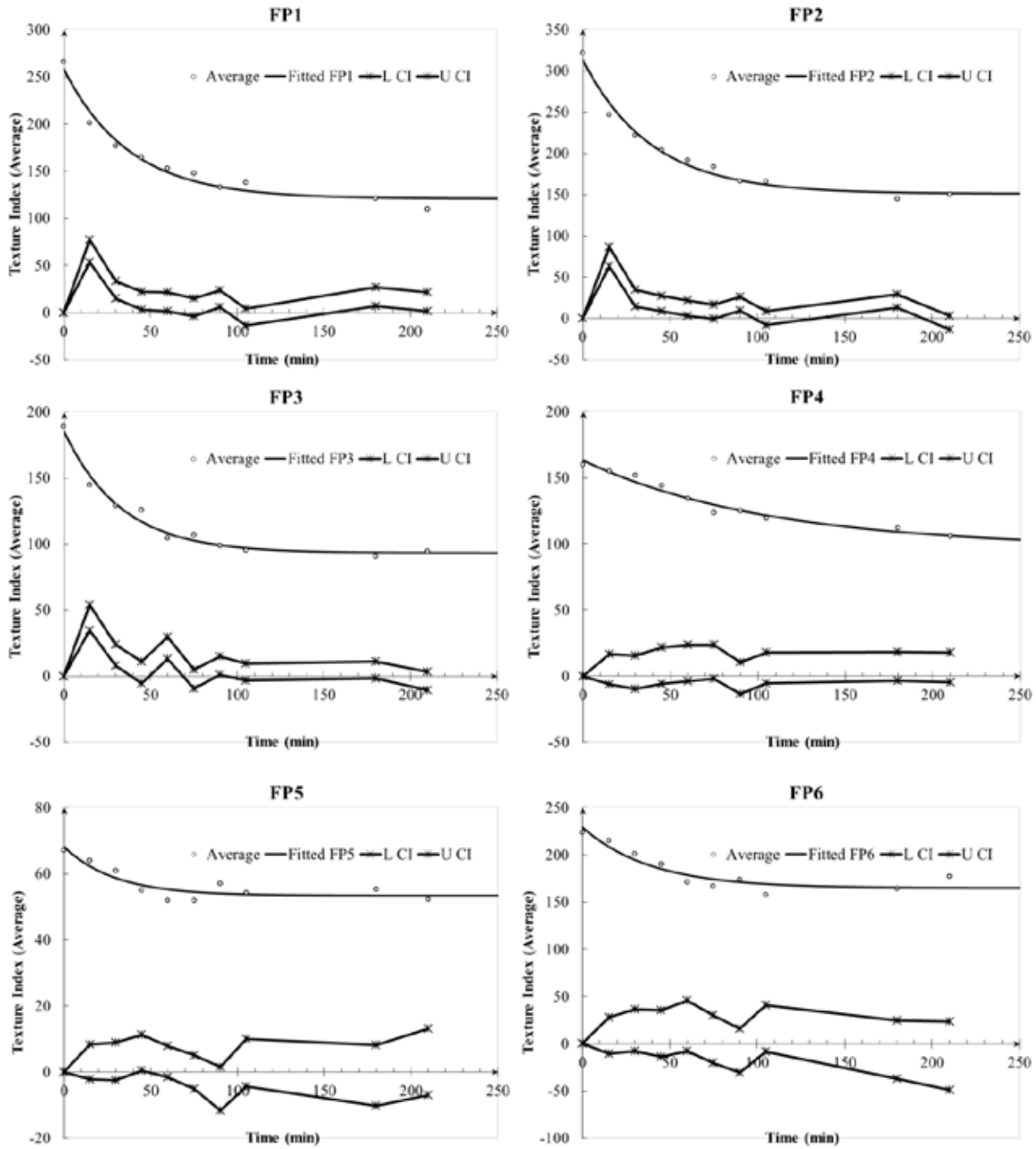


Figure 3.11 Averages of texture index, fitted curves, and confidence intervals [Stage 3].

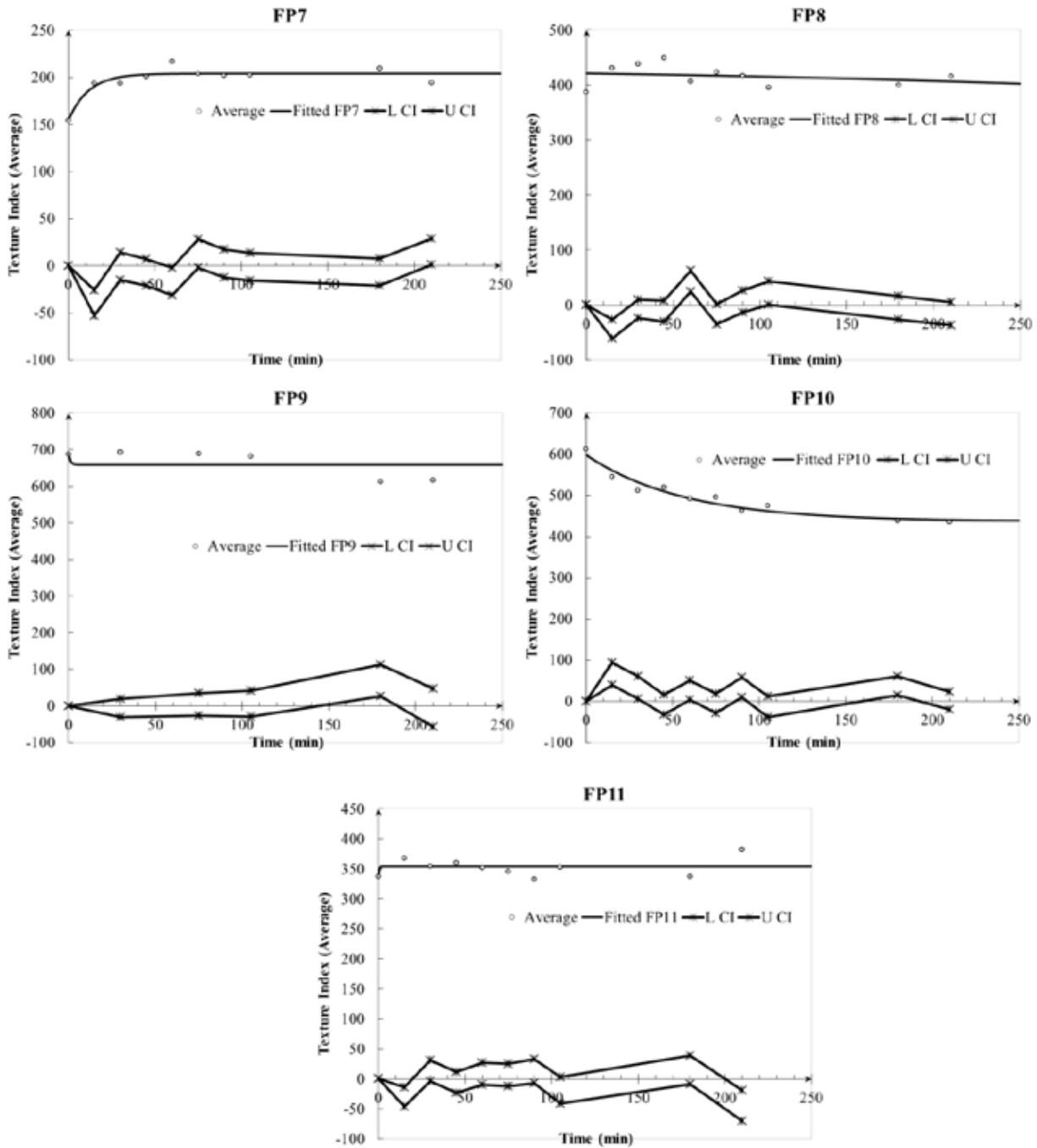


Figure 3.11 Averages of texture index, fitted curves, and confidence intervals [Stage 3].

Table 3.8 Statistical Inference on the Texture Means

IDOT Sample	Time Micro-Deval [min]	No. Particles	Texture Average	Std. Dev.	Lower CI	Upper CI
FP1	0	338	266.31	90.96		
	15	333	200.96	62.84	53.54	77.16
	30	309	176.84	57.91	14.78	33.46
	45	286	164.27	60.52	3.03	22.10
	60	274	153.07	60.38	1.19	21.22
	75	265	147.67	50.92	-4.01	14.82
	90	243	133.19	51.87	5.53	23.43
	105	225	138.02	48.87	-13.96	4.30
	180	184	121.15	51.36	7.07	26.65
	210	194	109.70	47.09	1.50	21.40
FP2	0	353	321.77	87.42		
	15	318	246.99	69.24	62.90	86.66
	30	292	222.31	58.39	14.54	34.82
	45	310	204.49	57.64	8.55	27.10
	60	263	192.08	53.24	3.32	21.50
	75	279	183.80	48.82	-0.33	16.90
	90	229	166.29	47.21	9.12	25.88
	105	246	165.95	45.24	-7.98	8.67
	180	195	144.94	41.77	12.87	29.15
	210	168	150.24	39.07	-13.63	3.02
FP3	0	317	189.23	67.01		
	15	323	144.81	55.68	34.86	53.97
	30	285	128.82	42.64	8.16	23.83
	45	253	125.99	54.37	-5.51	11.15
	60	236	104.57	38.21	13.13	29.70
	75	218	106.80	39.89	-9.43	4.97
	90	217	98.77	34.07	1.06	15.00
	105	196	95.51	32.86	-3.19	9.72
	180	173	90.79	30.44	-1.74	11.18
	210	142	94.48	32.52	-10.70	3.32
FP4	0	320	159.80	73.96		
	15	351	154.72	75.05	-6.20	16.37
	30	314	151.95	89.03	-9.83	15.36
	45	315	144.06	87.73	-5.92	21.71
	60	288	134.33	82.75	-3.88	23.34
	75	263	123.64	70.34	-2.10	23.48
	90	264	125.29	70.06	-13.64	10.34
	105	262	119.28	64.34	-5.48	17.51
	180	227	111.99	56.87	-3.46	18.03
	210	206	105.61	62.69	-4.93	17.69
FP5	0	492	67.10	38.33		
	15	388	64.04	40.00	-2.17	8.28
	30	304	60.89	36.75	-2.58	8.89
	45	238	55.04	27.05	0.47	11.22
	60	180	51.96	21.96	-1.61	7.79
	75	135	51.98	23.39	-5.11	5.06

IDOT Sample	Time Micro-Deval [min]	No. Particles	Texture Average	Std. Dev.	Lower CI	Upper CI
	90	135	57.09	31.07	-11.66	1.46
	105	107	54.26	25.65	-4.32	9.98
	180	49	55.27	28.00	-10.23	8.21
	210	25	52.17	15.99	-6.94	13.13
FP6	0	469	223.52	138.37		
	15	363	215.04	144.22	-10.93	27.90
	30	240	200.79	131.14	-8.01	36.50
	45	222	190.03	137.84	-13.82	35.34
	60	189	171.27	137.39	-7.93	45.46
	75	205	166.60	114.29	-20.41	29.73
	90	186	174.05	122.01	-30.94	16.05
	105	161	157.88	113.00	-8.58	40.91
	180	110	164.26	137.35	-37.42	24.66
	210	102	177.25	132.58	-49.34	23.35
FP7	0	378	154.31	84.72		
	15	378	193.63	104.61	-52.89	-25.75
	30	375	193.83	99.71	-14.80	14.39
	45	372	200.71	94.67	-20.82	7.06
	60	378	217.33	107.74	-31.14	-2.12
	75	366	204.30	105.06	-2.26	28.32
	90	360	201.80	101.81	-12.54	17.56
	105	368	202.70	98.51	-15.47	13.65
	180	352	209.50	98.15	-21.16	7.57
	210	349	194.56	87.54	1.17	28.70
FP8	0	248	387.21	107.04		
	15	249	430.73	87.61	-60.72	-26.32
	30	254	438.23	101.43	-24.05	9.06
	45	241	449.44	113.88	-30.24	7.82
	60	246	406.16	97.93	24.39	62.15
	75	236	422.97	107.42	-35.18	1.57
	90	217	416.66	109.65	-13.71	26.32
	105	234	395.03	119.71	0.46	42.80
	180	211	400.02	110.94	-26.43	16.44
	210	211	415.73	107.15	-36.52	5.11
FP9	0	423	688.27	162.32		
	30	304	693.68	176.62	-30.58	19.76
	75	218	689.38	176.81	-26.44	35.04
	105	186	682.80	185.67	-28.96	42.11
	180	131	612.60	198.61	26.97	113.42
	210	101	617.07	202.02	-56.51	47.58
FP10	0	387	613.08	194.62		
	15	366	546.04	186.71	39.80	94.27
	30	341	512.41	174.50	7.01	60.26
	45	341	520.04	151.66	-32.17	16.91
	60	324	492.06	156.27	4.55	51.40
	75	333	496.72	145.40	-27.75	18.44
	90	331	462.82	169.56	9.87	57.94

IDOT Sample	Time Micro-Deval [min]	No. Particles	Texture Average	Std. Dev.	Lower CI	Upper CI
FP11	105	310	475.41	153.75	-37.62	12.44
	180	296	437.87	134.08	14.60	60.48
	210	295	435.73	135.21	-19.57	23.86
	0	389	337.54	107.16		
	15	315	367.73	110.28	-46.37	-14.01
	30	271	354.19	109.23	-4.28	31.36
	45	248	360.16	97.67	-23.77	11.83
	60	225	351.73	102.79	-9.69	26.54
	75	205	345.46	94.68	-12.39	24.94
	90	176	332.99	103.91	-7.62	32.56
	105	159	352.32	104.73	-41.70	3.05
180	127	337.58	98.28	-8.86	38.34	
210	108	382.08	99.74	-69.92	-19.09	

The rate of texture loss as a function of Micro-Deval polishing time was also investigated. An example of the rate of texture loss is shown in Figure 3.12 which depicts aggregate source FP1; the rate is presented as the percent change in texture per minute with positive values representing the loss of texture. The figure clearly indicates that the rate of texture loss decreases with the increase in Micro-Deval polishing time and reaches a near-zero constant value around 210 minutes, which proves that even though the CI analysis for FP1 did not satisfy the terminal texture hypothesis (CI contain zero at 210 minutes), the drop of texture loss rate to near-zero value indicates that the aggregate reached its terminal texture. A closer look at the polishing curves indicate that the increase in aggregate texture and/or aggregate texture fluctuation was observed in sources FP7, FP8, FP9, and FP11, which explains the low texture polishing R-squared values for some of these samples. A similar behavior was documented in previous studies (Mahmoud and Masad 2007, Rezaei et al. 2009) and can be attributed to one of the following reasons: 1) particles break instead of being polished, thus exposing their internal surface texture, 2) the aggregate is hard to polish, having strong granular structure (FP8 & FP9), 3) the polishing mechanism in Micro-Deval exposes a more textured surface covered with a smoother surface (FP7), 4) the mineralogy of some aggregates such as sandstone continuously exposes a new textured surface with polishing (FP11), or 5) the aggregate texture is low, and therefore polishing in Micro-Deval will not have the expected effect.

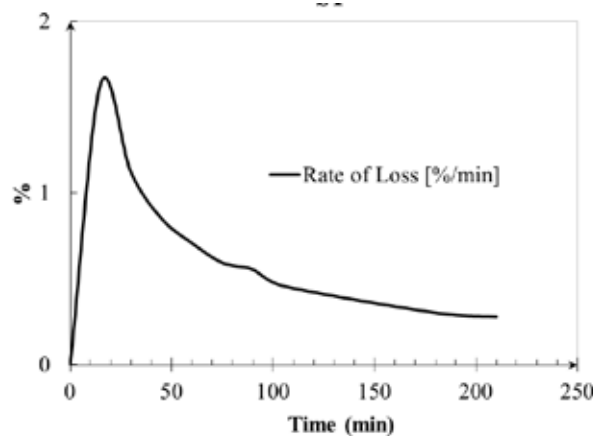


Figure 3.12 Rate of texture loss for different polishing time – FP1.

3.2.4 Stage 4: Procedure Simplification

The procedure described in the previous section requires testing nine samples in the Micro-Deval and scanning ten samples in AIMS (including before-polishing samples), to describe aggregate polishing behavior with less intensive lab work. Mahmoud and Masad (2007) suggested that the analytical model describing aggregate polishing can be obtained from three data points without sacrificing the accuracy of the model. A similar approach was followed in this study by fitting the model to four polishing points: 0, 60, 105 and 210 minutes; the 0 and 210 were selected to capture the initial and terminal texture. Figure 3.11 indicates that, for the majority of aggregate samples, the polishing curves started to plateau around the 105-minutes point, while the 60-minutes point was selected to represent the initial part of the polishing curve. In addition to the 4-point model, a 3-point model was also investigated (0, 105, and 210 minutes). Figure 3.13 illustrates the curves for fitting the analytical model for all ten, three, and four points. Figure 3.13 shows that both the 3-point and 4-point models give similar fitting functions to the 10-points model. The 4-point model provides a more accurate curve; however, the 3-point model provides an acceptable approximation of the 10-point model and is considered more practical and requires less laboratory testing.

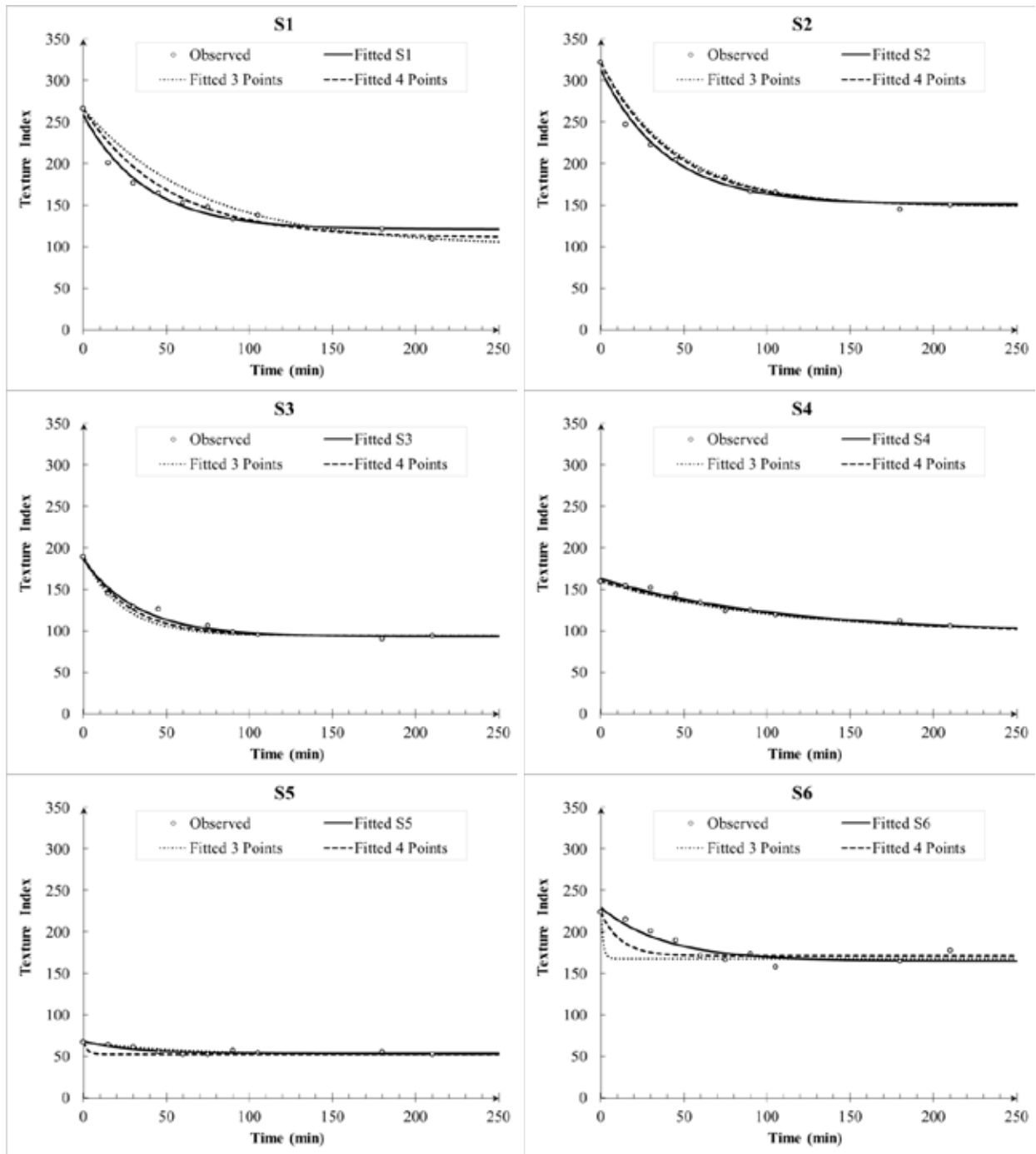


Figure 3.13 Fitted model based on texture index and considering all, three, and four data points.

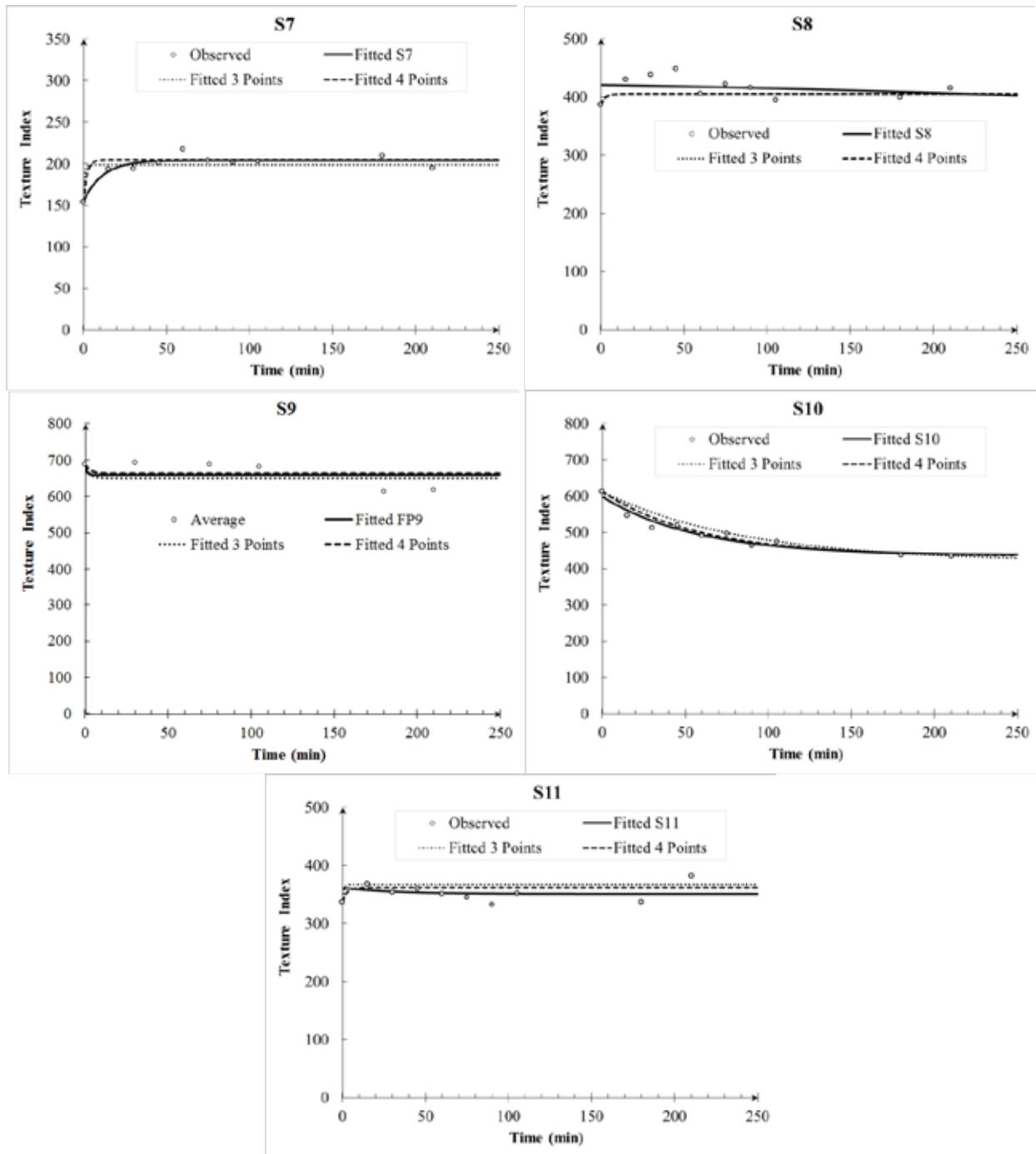


Figure 3.13 Fitted model based on texture index and considering all, three, and four data points.

3.2.5 Stage 5: Procedure Extension

The next analysis focused on extending the procedure to aggregate angularity. The same analysis procedure was applied to aggregate angularity. Figure 3.14 shows a summary of the loss in angularity under different Micro-Deval degradation intervals. It is evident that the analytical model used for describing texture changes can also be used to represent the angularity property. The angularity

degradation curves and the CI-lines clearly indicate that the aggregate materials tested reached their terminal angularity values at or before 210 minutes in the Micro-Deval.

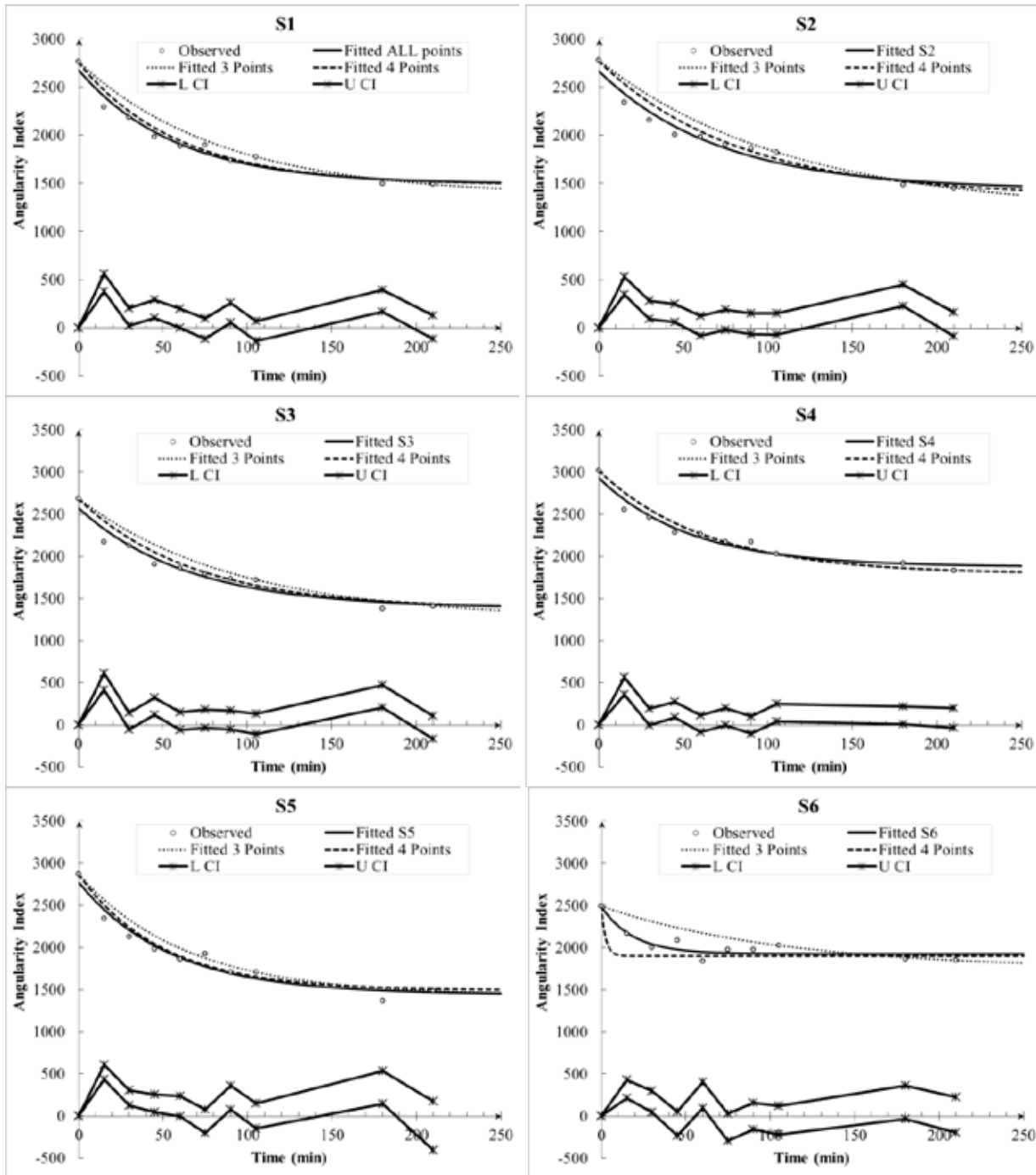


Figure 3.14 Fitted model based on angularity index and considering all, three, and four data points.

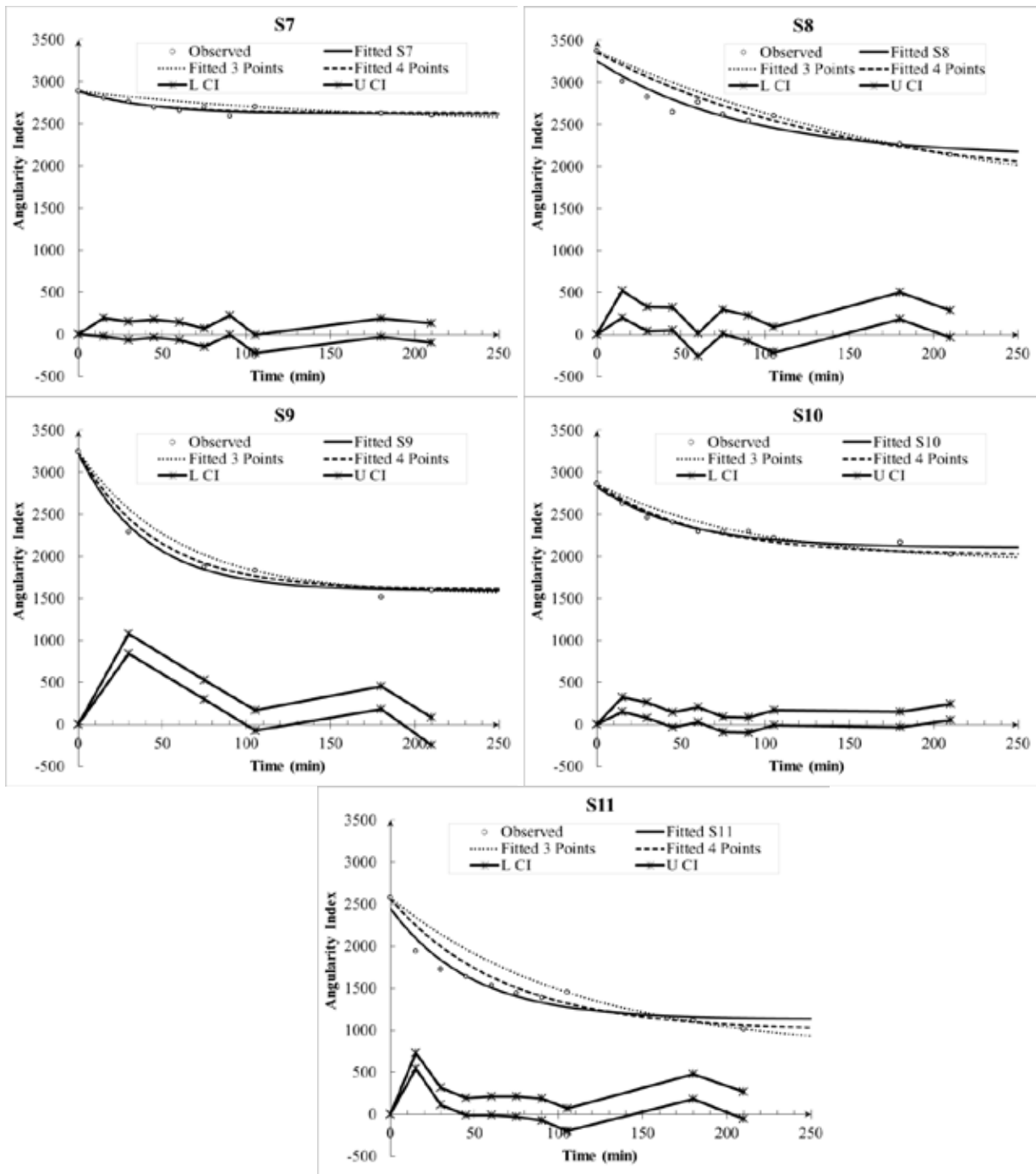


Figure 3.14 Fitted model based on angularity index and considering all, three, and four data points.

3.3 AIMS & E-UIAIA DATABASE

As recommended in Stage 4, aggregate polishing properties could be measured by measuring shape properties for aggregate before polishing and at 105 and 210 minutes of polishing in the Micro-Deval. A database was developed to summarize the testing results of this research study. Each aggregate source was labeled with a sample # starting with 001 and increasing by 1. Two samples were considered from each source, and the before- Micro-Deval properties were then measured on one of the samples. Based on the recommendations of this study, only 120 aggregate particles are required. The first sample, S1, was polished for 105 minutes while the second sample, S2, was polished for 210 minutes. The polished samples were scanned with AIMS to obtain the after- Micro-Deval properties. In addition to that, Micro-Deval sample weights and weight losses were also recorded. Table 3.9 shows the general outline of the database. The database was delivered to IDOT electronically in Microsoft Excel format. A similar database was developed for the E-UIAIA results as illustrated in Table 3.10.

Table 3.9 AIMS- Micro-Deval Database Format

SAMPLE #	SUB-SAMPLE	# PARTICLES	BMD-0MIN				# PARTICLES	AMD (S1: 105 AND S2: 210)				Micro-Deval		
			SHAPE PROPERTIES					SHAPE PROPERTIES				WEIGHT BEFORE	WEIGHT AFTER	WEIGHT LOSS
			ANGULARITY		TEXTURE			ANGULARITY		TEXTURE				
			Avg.	Std. Dev.	Avg.	Std. Dev.		Avg.	Std. Dev.	Avg.	Std. Dev.	gr	gr	%
001	S1	336	1409.9	905.4	154.4	108.5	283	1264.7	850.6	145.2	117.8	750.6	704.4	6.16
	S2	319	1375.0	902.4	157.6	111.1	120	1467.6	600.3	94.33	42.53	750.6	704.4	6.16
002	S1	306	2843.1	628.7	207.8	63.7	221	1773.6	591.7	111.3	42.40	749.4	638.4	14.81
	S2	306	2791.1	630.2	203.4	69.2	120	1075.0	883.1	127.4	109.2	749.4	638.4	14.81

Table 3.10 E-UIAIA- Micro-Deval Database Format

SAMPLE #	BMD-0MIN			AMD-105MIN			AMD-210MIN		
	# PARTICLES	ANGULARITY	TEXTURE	# PARTICLES	ANGULARITY	TEXTURE	# PARTICLES	ANGULARITY	TEXTURE
001	336	290	1.7	283	306	1.85	120	172	0.96
002	306	456	2.55	221	303	1.78	120	217	1.33

CHAPTER 4 SUMMARY AND IMPLEMENTATION RECOMMENDATIONS

4.1 SUMMARY

Eleven coarse aggregate samples from different sources were subjected to polishing in the Micro-Deval apparatus at nine different time intervals. Aggregate surface texture was characterized for different Micro-Deval polishing time intervals using AIMS and E-UIAIA image analysis test devices. Confidence interval analysis was used to determine Micro-Deval polishing time required to reach aggregate terminal texture by comparing surface texture of consecutive polishing intervals in Micro-Deval, based on the hypothesis that terminal texture is reached when CI contains zero. It was observed that the aggregates tested in this study reached terminal texture after 210 minutes of polishing in Micro-Deval. The main findings from this study are as follows:

- Aggregates were partially polished for different time intervals going from 15 -180 min in the Micro-Deval. It was concluded by statistical analysis that some aggregates did not reach their terminal texture values at 180 minutes in the Micro-Deval as reported in the literature. This was expected because of the modification of the aggregate weight and size in the Micro-Deval
- Analyses of the aggregate polishing curves proved that Micro-Deval-AIMS procedure is sufficient to assess the terminal texture of coarse aggregates at 210 minutes.
- Aggregates with different mineralogy exhibited different textural polishing and retention characteristics.
- The full polishing curve could be accurately estimated using only three texture points: 0, 105, and 210 minutes. However, a fourth texture point could be used (60 minutes) to obtain a more precise approximation.
- Polishing curves could be mathematically formulated: the model parameters in the regression equation described the initial texture, $a+b$; terminal texture, a ; and the rate of texture loss, c .
- 77 aggregate sources were scanned before polishing and after 105 and 210 Micro-Deval polishing minutes to develop the aggregate-AIMS database for IDOT.

4.2 IMPLEMENTATION RECOMMENDATIONS

4.2.1 Polishing Procedure

Based on the results and analyses of this research project data, the following procedure is recommended to characterize coarse aggregate polishing:

1. Obtain two 750-g coarse aggregate samples passing the 1/2 in. sieve and retained on the 3/8 in. sieve
2. Measure aggregate initial surface texture with AIMS (texture at 0-minute polishing)
3. Subject one sample to polishing in Micro-Deval:
 - a. Soak the aggregate sample in 2 liters of water for at least 60 minutes in Micro-Deval drum;

- b. Add a charge of 5,000 grams of 9.5 mm diameter steel balls;
 - c. Subject the aggregate sample to polishing in the Micro-Deval for 105 minutes;
 - d. Wash and sieve the aggregate sample retained on the #16 sieve;
 - e. Oven dry sample and obtain material retained on the 3/8 in. sieve; and
 - f. Measure aggregate surface texture with AIMS (texture at 105 minutes polishing).
4. Repeat step 3 for the second aggregate sample to obtain aggregate surface texture at 210 minutes by changing the time in 3-c to 210 minutes.
 5. If a 4-point polishing curve is desired, repeat step 3 for a third sample to obtain the surface texture at 60 minutes by changing the time in 3-c to 60 minutes.

4.2.2 Database

The research team highly recommends that IDOT continue measuring aggregate properties before polishing and after 105 and 210 minutes of polishing in the Micro-Deval and update the database developed in this study on a regular basis. This database is valuable for identifying aggregates for high friction surface courses and for verifying the procedure developed in this study.

4.2.3 Procedure Validation

The procedure developed in this study compared very well with historical laboratory friction data obtained by IDOT; however, it is recommended that a one-to-one comparison be conducted for several aggregate sources to directly compare AIMS-Micro-Deval and VST results.

REFERENCES

- Al-Rousan, T. M. 2004. *Characterization of Aggregate Shape Properties Using a Computer Automated System*. Ph.D. Dissertation, Texas A&M University, College Station, TX.
- Al-Rousan, T., E. Masad, E. Tutumluer, and T. Pan. 2007. "Evaluation of Image Analysis Techniques for Quantifying Aggregate Shape Characteristics." *Journal of Construction and Building Materials* 21:978–990.
- Al-Rousan, T., E. Masad, L. Myers, and C. Speigelman. 2005. "New Methodology for Shape Classification of Aggregates." *Transportation Research Record* 1913:11–23.
- Barksdale, R. D., C. O. Pollard, T. Siegel, and S. Moeller. 1992. *Evaluation of the Effect of Aggregate on Rutting and Fatigue of Asphalt*. Technical Report FHWAAG- 92-8812. Atlanta: Georgia Department of Transportation.
- Bloem, D. 1971. "Skid Resistance—The Role of Aggregates and Other Factors." *National Sand and Gravel Association Circular* 109:1–30.
- Boler, H., M. Wnek, and E. Tutumluer. 2012. "Establishing Linkages Between Ballast Degradation and Imaging Based Aggregate Particle Shape, Texture and Angularity Indices," pp. 37–38. *Proceedings of the 2nd International Conference on Transportation Geotechnics*. CRC Press, London, 2012.
- Brzezicki, J. M., and J. Kasperkiewicz. 1999. "Automatic Image Analysis in Evaluation of Aggregate Shape." *ASCE Journal of Computing in Civil Engineering (Special Issue on Image Processing)* 13(2):123–130.
- Chowdhury, A., J. W. Button, V. Kohale, and D. Jahn. 2001. *Evaluation of Superpave Fine Aggregate Angularity Specification*. International Center for Aggregates Research ICAR Report 201-1. Texas Transportation Institute. College Station: Texas A&M University.
- Cooley, L. Jr., and R. James. 2003. "Micro-Deval Testing of Aggregates in the Southeast." *Transportation Research Record* 1837:73–79.
- Crouch, L., J. Gothard, G. Head, and W. Goodwin. 1995. "Evaluation of Textural Retention of Pavement Surface Aggregates." *Transportation Research Record* 1486:124–129.
- Dahir, S. 1979. "A Review of Aggregate Selection Criteria for Improved Wear Resistance and Skid Resistance of Bituminous Surfaces." *Journal of Testing and Evaluation* 7:245–253.
- Fletcher, T., C. Chandan, E. Masad, and K. Sivakumar. 2003. "Aggregate Imaging System (AIMS) for Characterizing the Shape of Fine and Coarse Aggregates." *Transportation Research Record* 1832:67–77.
- Forster, S. W. 1989. "Pavement Microtexture and its Relation to Skid Resistance." *Transportation Research Record* 1215:151–164.
- Gatchalian, D. 2005. *Characterization of Aggregate Resistance to Degradation in Stone Matrix Asphalt Mixtures*. MS Thesis, Texas A&M University, College Station, TX.
- Gatchalian, D., E. Masad, A. Chowdhury, and D. Little. 2006. *Characterization of Aggregate Resistance to Degradation in Stone Matrix Asphalt Mixtures*. International Center for Aggregate Research, Report 204-1F.
- Gates L. L. 2010. *Experimental Evaluation of New Generation Aggregate Image Measurement System*. MS Thesis, Texas A&M University, College Station, TX.

- Gates, L., E. Masad, R. Pyle, and D. Bushee. 2011. *Aggregate Imaging Measurement System 2 (AIMS-II): Final Report*. Highway for Life Technology Partnership Program, Federal Highway Administration, US Department of Transportation.
- Gonzalez, R.C., R.E. Woods, and S.L. Eddins. 2009. pp. 444–454. In *Digital Image Processing Using MATLAB*. USA: Gatesmark Publishing.
- Hryciw, R. D., and S. A. Raschke. 1996. "Development of a Computer Vision Technique for In-Situ Soil Characterization." *Transportation Research Record* 1526:86–97.
- Indraratna, B., and W.S. Salim. 2005. pp. 28–30. In *Mechanics of Ballasted Rail Tracks A Geotechnical Perspective*. Taylor & Francis. London:
- Janoo, V. C. 1998. *Quantification of Shape, Angularity, and Surface Texture of Base Course Materials*. U.S. Army Corps of Engineers Special Report 98-1. Hanover, NH: Cold Regions Research & Engineering Laboratory.
- Kandhal, P. S., J. B. Motter, and M. A. Khatri. 1991. "Evaluation of Particle Shape and Texture: Manufactured Versus Natural Sands." *Transportation Research Record* 1301:48–67.
- Kandhal, P., and F. Jr. Parker. 1998. *Aggregate Tests Related to Asphalt Concrete Performance in Pavements*. National Cooperative Highway Research Program Report 405. Washington, D.C.: Transportation Research Board, National Research Council.
- Kuo, C. Y., J. D. Frost, J. S. Lai, and L. B. Wang. 1996. "Three-Dimensional Image Analysis of Aggregate Particle from Orthogonal Projections." *Transportation Research Record* 1526:98–103.
- Kuo, C., and R. B. Freeman. 2000. "Imaging Indices for Quantification of Shape, Angularity, and Surface Texture of Aggregates." *Transportation Research Record* 1721:57–65.
- Lane, B., C. Rogers, and S. Senior. 2000. "The Micro-Deval Test for Aggregates in Asphalt Pavement." *Presented at the 8th Annual Symposium of International Center for Aggregate Research*, Denver, CO, 2000.
- Lane, S., C. Druta, L. Wang, and W. Xue. 2011. "Modified Micro-Deval Procedure For Evaluating the Polishing Tendency of Coarse Aggregates." *Transportation Research Record* 2232:34–43.
- Li, L., P. Chan, D. G. Zollinger, and R. L. Lytton. 1993. "Quantitative analysis of aggregate shape based on fractals." *ACI Materials Journal* 90(4):357–365.
- Luce A. D. 2006. *Analysis of Aggregate Imaging System (AIMS) Measurements and Their Relationship to Asphalt Pavement Skid Resistance*. MS Thesis, Texas A&M University, College Station, TX.
- Luce, A., E. Mahmoud, E. Masad, and A. Chowdhury. 2007. "Relationship of Aggregate Microtexture to Asphalt Pavement Skid Resistance." *Journal of Testing and Evaluation*, ASTM 35(6):578–588.
- Lynn, T., R.S. James, P.Y. Wu, and D.M. Jared. 2007. "Effect of Aggregate Degradation on Volumetric Properties of Georgia's Hot-Mix Asphalt." *Transportation Research Record* 1998:123–131.
- Maerz, N. H., and W. Zhou. 2001. "Flat and Elongated: Advances Using Digital Image Analysis." In *Proceedings of the 9th Annual Symposium of the International Center for Aggregates Research (ICAR)*, Austin, TX, 2001.
- Mahmoud, E., and E. Masad. 2007. "Experimental Methods for the Evaluation of Aggregate Resistance to Polishing, Abrasion and Breakage." *Journal of Materials in Civil Engineering*, ASCE 19(11):977–985.
- Mahmoud, E., L. Gates, E. Masad, S. Erdogan, and E. Garboczi. 2010. "Comprehensive Evaluation of AIMS Texture, Angularity, and Dimension Measurements." *Journal of Materials in Civil Engineering* 22(4).

- Mahmoud, E.M. 2005. *Development of Experimental Method for the Evaluation of Aggregate Resistance to Polish, Abrasion, and Breakage*. M.S. Thesis, Texas A&M University, College Station, TX.
- Masad, E. 2003. *The Development of a Computer Controlled Image Analysis System for Measuring Aggregate Shape Properties*. NCHRP-IDEA Program, Project 77 Final Report. Washington, D.C.: Transportation Research Board, National Research Council.
- Masad, E. A., B. Muhunthan, N. Shashidhar, and T. Harman. 1999b. "Effect of Compaction Procedure on the Aggregate Structure in Asphalt Concrete." *Transportation Research Record* 1681:179–184.
- Masad, E., and J. Button. 2000. "Unified Imaging Approach for Measuring Aggregate Angularity and Texture." *Journal of Computer-Aided Civil and Infrastructure Engineering* 15(4):273–280.
- Masad, E., B. Muhunthan, N. Shashidhar, and T. Harman. 1999a. "Internal Structure Characterization of Asphalt Concrete Using Image Analysis." *ASCE Journal of Computing in Civil Engineering (Special Issue on Image Processing)* 13(2):88–95.
- Masad, E., D. Olcott, T. White, and L. Tashman. 2001. "Correlation of Fine Aggregate Imaging Shape Indices with Asphalt Mixture Performance." *Transportation Research Record* 1757:148–156.
- Masad, E., J. Button, and T. Papagiannakis. 2000. "Fine Aggregate Angularity: Automated Image Analysis Approach." *Transportation Research Record* 1721:66–72.
- Masad, E., T. Al-Rousan, J. Button, D. Little, and E. Tutumluer. 2007. *Test Methods for Characterizing Aggregate Shape, Texture, and Angularity*. Washington, D.C.: National Cooperative Highway Research Program NCHRP Report 555.
- McGahan, J. 2005. *The Development of Correlations Between HMA Pavement Performance and Aggregate Shape Properties*. MS Thesis, Texas A&M University, College Station, TX.
- Meininger, R. (2004). "Micro-Deval vs. L.A. Abrasion." *Rock Products* 10735.
- Moaveni, M., Wang, S., Hart, J. M., Tutumluer, E., Ahuja, N., "Aggregate Size and Shape Evaluation Using Segmentation Techniques and Aggregate Image Processing Algorithms", *Journal of Transportation Research Record*, No. 2335, pp. 50–59, 2013, Washington DC, USA
- Moavenzadeh, F., and W. H. Goetz. 1963. *Aggregate Degradation In Bituminous Mixtures: Technical Paper*. Publication FHWA/IN/JHRP-63/05. Joint Transportation Research Program, Indiana Department of Transportation and Purdue University.
- Page, G.C., J.A. Musselman, and D.C. Romano. 1997. "Effects of Aggregate Degradation on Air Voids of Structural Asphalt Mixture in Florida." *Transportation Research Record* 1583:19–27.
- Pan, T., 2006. *Investigation of Coarse Aggregate Morphology Affecting Hot Mix Behavior Using Image Analysis*. Ph.D. Dissertation, University of Illinois, Urbana Champaign, IL.
- Pan, T., and E. Tutumluer. 2010. "Imaging-Based Direct Measurement of Aggregate Surface Area and its Application in Asphalt Mixture Design." *International Journal of Pavement Engineering* 11(5).
- Pintner, R.M., T.S. Vinson, and E.G. Johnson. 1987. "Nature of Fines Produced in Aggregate Processing." *ASCE Journal of Cold Regions Engineering* 1(1):10–12.
- Rao, C., E. Tutumluer, and I.T. Kim. 2002. "Quantification of Coarse Aggregate Angularity Based on Image Analysis." *Transportation Research Record* 1787:117–124.
- Rogers, C. 1998. "Canadian Experience with the Micro-Deval Test for Aggregates." *Advances in Aggregates and Armourstone Evaluation* 13:139–147.

- Senior, S. and C. Rogers. 1991. "Laboratory Tests for Predicting Coarse Aggregate Performance in Ontario." *Transportation Research Record* 1301:97–106.
- Singh, D., M. Zaman, and S. Commuri. 2013. "Effect of Production and Sample Preparation Methods on Aggregate Shape Parameters." *International Journal of Pavement Engineering* 14(2).
- Tutumluer, E. and T. Pan. 2008. "Aggregate Morphology Affecting Strength and Permanent Deformation Behavior of Unbound Aggregate Materials." *Journal of Materials in Civil Engineering* 20(9):617–627.
- Tutumluer, E., C. Rao, and J. Stefanski. 2000. *Video Image Analysis of Aggregates*. Final Project Report FHWA-IL-UI-278. Civil Engineering Studies UILU-ENG- 2000-2015. Urbana-Champaign: University of Illinois.
- Wang, L. B., and J. S. Lai. 1998. "Quantify Specific Surface Area of Aggregates Using an Imaging Technique." *Transportation Research Board 77th Annual Meeting*, Washington, D.C., 1998.
- Wang, L., W. Sun, E. M. Lally, A. Wang, C. Druta, and E. Tutumluer. 2012. Application of LADAR in the Analysis of Aggregate Characteristics. National Cooperative Highway Research Program Report 724. Washington, D.C.: Transportation Research Board, National Research Council.
- Weingart, R. L., and Prowell, B. D. 1999. "Specification development using the VDG-40 Videograder for shape classification of aggregates." *Proceedings of the 7th Annual Symposium of the International Center for Aggregate Research (ICAR)*, University of Texas, Austin, TX, 1999.
- Wilson, J. D., and L. D. Klotz. 1996. "Quantitative Analysis of Aggregates Based on Hough Transform." *Transportation Research Record* 1530:111–115.
- Wu, Y., F. Parker, and P. Kandhal. 1998. "Aggregate Toughness/Abrasion Resistance and Durability/Soundness Tests Related to Asphalt Concrete Performance in Pavements." *Transportation Research Record* 1638:85–93.
- Yeggoni, M., J. W. Button, and D. G. Zollinger. 1994. *Influence of Coarse Aggregate Shape and Surface Texture on Rutting of Hot-Mix Concrete*. Texas Transportation Institute Report 1244-6. College Station: Texas A&M University.

